LA-UR-17-25579
Approved for public release; distribution is unlimited.

Title: Candidate Low-Temperature Glass Waste Forms for Technetium-99 Recovered from Hanford Effluent Management Facility Evaporator Concentrate

Author(s): Ding, Mei
Tang, Ming
Rim, Jung Ho
Chamberlin, Rebecca M.

Intended for: Report

Issued: 2017-07-24 (rev.1)

Candidate Low-Temperature Glass Waste Forms for Technetium-99 Recovered from Hanford Effluent Management Facility Evaporator Concentrate

Mei Ding, Ming Tang, Jung Rim and Rebecca M. Chamberlin

July 11, 2017
LA-UR-17-25579

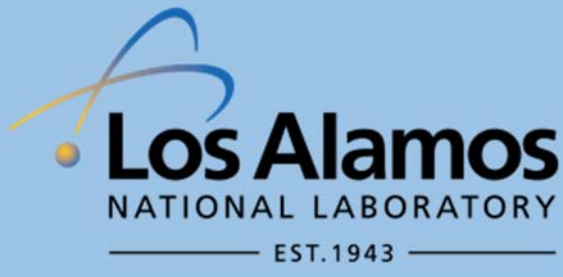

Candidate Low-Temperature Glass Waste Forms for Technetium-99 Recovered from Hanford Effluent Management Facility Evaporator Concentrate

Mei Ding, Ming Tang, Jung Rim, and Rebecca M. Chamberlin*

Executive Summary

Alternative treatment and disposition options may exist for technetium-99 (^{99}Tc) in secondary liquid waste from the Hanford Direct-Feed Low-Activity Waste (DFLAW) process. One approach includes development of an alternate glass waste form that is suitable for on-site disposition of technetium, including salts and other species recovered by ion exchange or precipitation from the EMF evaporator concentrate. By recovering the Tc content from the stream, and not recycling the treated concentrate, the DFLAW process can potentially be operated in a more efficient manner that lowers the cost to the Department of Energy.

This report provides a survey of candidate glass formulations and glass-making processes that can potentially incorporate technetium at temperatures <700 °C to avoid volatilization. Three candidate technetium feed streams are considered: (1) dilute sodium pertechnetate loaded on a non-elutable ion exchange resin; (2) dilute sodium-bearing aqueous eluent from ion exchange recovery of pertechnetate, or (3) technetium(IV) oxide precipitate containing Sn and Cr solids in an aqueous slurry. From the technical literature, promising candidate glasses are identified based on their processing temperatures and chemical durability data. The suitability and technical risk of three low-temperature glass processing routes (vitrification, encapsulation by sintering into a glass composite material, and sol-gel chemical condensation) for the three waste streams was assessed, based on available low-temperature glass data. For a subset of candidate glasses, their long-term thermodynamic behavior with exposure to water and oxygen was modeled using Geochemist's Workbench, with and without addition of reducing stannous ion.

For further evaluation and development, encapsulation of precipitated TcO2/Sn/Cr in a glass composite material based on lead-free sealing glasses is recommended as a high priority. Vitrification of pertechnetate in aqueous anion exchange eluent solution using a high lead content borate glass, or other low melting glass is also recommended for further evaluation and development. Additional laboratory studies of phase behavior and chemical durability of low-temperature glasses is also recommended to provide risk mitigation if one of the primary development paths proves infeasible. This report is a deliverable for the task "Candidate Low-T Glass Waste Forms for EMF Bottoms On-Site Disposition Alternative Option."

* Correspondence: rmchamberlin@lanl.gov

Table of Contents

List of Acronyms and Abbreviations

GCM	Glass Composite Material
CCIM	Cold Crucible Induction Melter/Melting
CTO	Chief Technology Office
DFLAW	Direct Feed Low Activity Waste
DI	De-ionized
EMF	Effluent Management Facility
GWB	Geochemist's Workbench
HLW	High Level Waste
IDF	Integrated Disposal Facility
JHM	Joule Heated Melter/Melting
KAERI	Korea Atomic Energy Research Institute
LAW	Low-Activity Waste
LDR	Land Disposal Requirements
MCC	Materials Characterization Center
mol	mole
PCT	Product Consistency Test
RCRA	Resource Conservation and Recovery Act
TCLP	Toxicity Characteristic Leaching Procedure
WRPS	Washington River Protection Solutions
wt	weight
WTP	Waste Treatment Plant

Introduction

Alternative treatment and disposition options may exist for technetium-99 (^{99}Tc) in secondary liquid waste from the Hanford Direct-Feed Low-Activity Waste (DFLAW) process. One opportunity for the DFLAW Effluent Management Facility (EMF) concentrate disposition includes the possibility of treating the liquid in two steps, first recovering the Tc in the concentrate, and then allowing the treated concentrate (less the Tc) to be solidified in a manner to meet Land Disposal Requirements (LDR) under the Resource Conservation and Recovery Act (RCRA) [40 CFR 268]. By recovering the Tc content from the stream, and not recycling the treated concentrate, the DFLAW process can potentially be operated in a more efficient manner that lowers the cost to the Department of Energy. Since the salts in the concentrate (e.g. sulfate, chloride) cause lower waste loadings, when these salts are not returned to the Low Activity Waste (LAW) facility, less glass production is required for the same amount of tank waste treatment. Successful development of such a waste form may simplify or enhance DFLAW operations and eliminate impacts from recycling of EMF bottoms.

One approach includes development of an alternate glass waste form that is suitable for on-site disposition of technetium, including salts and other species recovered by ion exchange or precipitation from the EMF evaporator concentrate. In this report, Los Alamos National Laboratory provides a survey of candidate glass formulations and glass-making processes that can incorporate technetium at temperatures <700 °C to avoid volatilization. Promising candidates are identified based on their processing temperatures and chemical durability. For a subset of candidates, their long-term thermodynamic behavior with exposure to water and oxygen is modeled using Geochemist's Workbench. Recommendations to support final decision-making for future laboratory testing of glass formulations, including Tc incorporation and performance under Integrated Disposal Facility (IDF) conditions, are provided. This report supports the Technology Maturation and Analysis Program for the Chief Technology Office (CTO) of Washington River Protection Solutions (WRPS) in identifying options for alternative treatments and dispositions for secondary liquid wastes from the DFLAW process.

Feed Streams

According to the Technology Development Group of the WRPS One System Chief Technology Office, recovery of the technetium stream from a Waste Treatment Plant (WTP) secondary liquid waste stream, post-EMF evaporation, may be done via three methods. These are: (1) ion exchange with a non-elutable resin like Purolite A-530E, (2) ion exchange with elutable resin Superlig-639, or (3) precipitation with stannous chloride. From literature and testing, the nominal characteristics of the three recovered Tc streams are noted in Table 1. Concentrations of Tc in Superlig-639 ion exchange eluate streams from Hanford tank waste samples vary widely, but the median of four samples in one study was 2.3 mol%, or 0.5 wt%, relative to sodium ion in a dilute aqueous solution [Westsik 2014]. The composition of the solid from stannous ion precipitation of technetium from simulated Hanford waste is 0.17 wt% technetium, 8.3 wt% chromium, and 45.0 wt% tin [Taylor-Pashow 2015].

Table 1. Nominal characteristics of recovered Tc streams, as provided by WRPS Technology Development Group.

Stream	Purolite A-530E resin (non-elutable)	Superlig-639 ion exchange eluate	Precipitated $TcO_2 \cdot 2H_2O$ using Sn^{2+}
Phase	Organic resin in a water slurry	Water solution with dissolved salts	Water slurry with precipitated solids
Key composition for disposal	Mass loaded with Na^+, K^+, Cl^-, NO_2^-, NO_3^-, SO_4^{-2} with trace mass amounts of Tc	Na^+, K^+, Cl^-, NO_2^-, NO_3^-, SO_4^{-2} with trace mass amounts of Tc	Cr, Sn, Tc solid phase with Tc being a small amount of the total mass

A default process for dispositioning the recovered Tc stream is to have it routed to the LAW facility to be incorporated into borosilicate glass. This high temperature process (~1150°C) typically liberates more than half of the technetium, which would then be recaptured in the melter condensate [Westsik 2014, Pegg 2015]. Technetium liberation has been closely linked to temperatures above 700°C [Darab 1996]. For example, essentially no losses are noted in sample preparation for ^{99}Tc analyses on calcined soils with preparation temperatures less than 700°C [Uchida 2001]. Research on technetium liberation during borosilicate melting showed that solid sodium pertechnetate ($NaTcO_4$) begins to decompose and volatilize when the melt reaches 600 °C [Childs 2015], and potassium pertechnetate can begin to liberate volatile technetium at 500-550 °C [Gibson 1993]. Therefore, although the temperature criterion for this study is set by WRPS at <700 °C, it is preferable to identify a glass-forming process that can operate at even lower temperatures.

Prior Work

There are lower melting glasses that have the potential to incorporate the salts and other species noted in the table, and to provide excellent long-term performance in a disposal environment. Lower-temperature glasses were evaluated in the 1990's for Hanford high-level waste (HLW) vitrification [Cao 1995]. This literature survey focused on alternatives to borosilicate glass that would provide improved tolerance for certain single-shell tank constituents, e.g. phosphorus, chromium and aluminum. Reduced melting temperatures and avoidance of RCRA elements were considered desirable, though secondary, characteristics for these alternative glasses. A small experimental effort delivered a new iron-aluminum-phosphate (Fe-Al-P) glass formulation with improved chemical durability and reduced melting temperatures compared to borosilicate, but the melting temperature of 900 °C for this glass is too high for the technetium secondary waste stream that is the subject of this report.

Substantially more work has been done in recent years to develop low-temperature glasses for a variety of optical, electronics, and waste immobilization applications. In this report, we survey and summarize the relevant characteristics of these glasses and provide recommendations for their future development as potential technetium waste forms.

Process and Material Requirements

The sitewide inventory of technetium-99 in Hanford tank waste is estimated at 26,000 Ci or 1500 kg [Robbins 2013, Serne 2014]. Assuming a fairly conservative mass loading of 10% of a technetium-bearing liquid eluate or precipitated solid waste into a bismuth or lead-based glass waste form with a density of 6000 kg/m^3 [Pan 1995, Ferro 2017], the entire Hanford inventory could be encapsulated in perhaps 1000 m^3 of glass. This amount does not require a high process throughput or large-volume melter. In fact, at this limited scale, batch glass-forming processes, and continuous small-scale processes other than vitrification, become viable.

Complete dissolution of technetium and other salts in the glass matrix is most straightforwardly achieved by vitrification in a joule-heated or induction melter. Ideally, vitrification produces a waste form that distributes the waste homogeneously throughout the glass, but crystallization and mixing effects can introduce compositional variability. Glass composite materials, on the other hand, are made by blending a solid waste stream (crystalline or amorphous) with a robust solid glass matrix, which is fused at an elevated temperature to form a monolith. The glass composite material (GCM) retains a microstructure within which the host and guest materials are present as distinct materials, but the weathering rate of the guest is designed to be limited by containment within the host. Glasses formed via chemical condensation reactions (i.e. sol-gel glass) may contain either type of microstructure. Given the objective of a low-temperature glass-forming process for technetium immobilization, each of these types of materials will be considered here in turn.

Durability Requirements

Waste forms for on-site disposition of technetium secondary wastes must be durable enough to contain the radionuclide, but specific performance criteria are not yet established. As the currently accepted waste form for Hanford HLW, borosilicate glass can serve as a useful benchmark for this study, although the requirements for borosilicate may differ from those for a Tc-only waste form. The current specification for Hanford LAW glass is that the normalized release of sodium, silicon, and boron shall be less than 2 g/m^2 using the Product Consistency Test (PCT-A) [DOE 2001]. This is equivalent to an average rate of about 0.3 g/m^2/day. For the purpose of initial identification of promising glass candidates with low temperature processing and high chemical durability, we have set the requirements that the reported rate of release of major elements from a low-temperature glass cannot be more than 10-100 times greater than what is allowed for borosilicate waste forms. Glass waste forms with proven durability in this range are further considered as candidates for further development and testing for technetium immobilization. The waste form must also meet the Non-Wastewater Standard in the RCRA Land Disposal Restrictions, as measured by TCLP [40CFR268].

Unfortunately, researchers who have investigated low-temperature glasses have not uniformly applied a glass durability test method with conditions equivalent to the PCT-A to their experimental materials. A variety of ad-hoc tests have been reported, often at reduced temperatures (ambient to 70 °C) or for extended times. Even at identical times and temperatures and normalizing for differences in glass mass to solution volume ratios, the PCT and MCC (Materials Characterization Center) tests are not directly comparable either, because the former requires a finely-ground powder with high surface area [ASTM

C1285] and the latter requires a low-surface area monolith [ASTM C1220]. Many other low-temperature glasses, including dozens of commercially available formulations, have never been tested for their chemical durability. The absence of published leach test results should not permanently rule out these glasses, because chemical durability can be surveyed quickly and inexpensively. Conversely, a host glass that has proven durability cannot be assumed to perform as well once sodium pertechnetate or technetium(IV) oxide waste streams have been incorporated, so durability testing of the final mixture is an essential development activity.

Low Temperature Glasses

Overview

The best known low-melting glasses are based on the lead borate (PbO-B_2O_3) system, with reported melting temperatures as low as 400-500 °C (Appendix A and B). Lead borosilicate glass has been developed for high temperature vitrification of radioactive waste in India, and it has proven to have excellent durability for this application [Raj 2006], but it does not meet the temperature criterion to be considered for this secondary waste stream. Other lead-based glasses are considered here as candidate glasses for low-temperature ^{99}Tc immobilization, provided they can be demonstrated to meet RCRA LDR requirements (0.75 mg/L TCLP). As one example, lead borate binary glass compositions with PbO content of 40-80 mol% have been shown to melt between 465-545 °C and possess good durability against leaching [Erdogan 2014]. These will be discussed in a later section.

There are four other important glass families that are well-described in the literature and that demonstrate potential to serve as low temperature waste forms: phosphate glass (P_2O_5 family), vanadate glass (V_2O_5 family), borate glass (B_2O_3 family), and bismuthate glass (Bi_2O_3 family). Melting temperatures of these glasses can be below 700 °C, providing a significant advantage for Tc disposition over existing borosilicate formulations. Unlike crystalline solids, glasses have no defined melting point, but instead continuously transform from the solid state to the viscous plastic state. Because of this, the experimental literature often does not report melting temperatures, and other descriptors of glass behavior are used. These include the transition temperature (T_g), the temperature at which the material initially behaves as a viscous, supercooled liquid instead of a rigid, brittle solid [ASTM C965]. Next, the softening temperature (T_f) is the maximum temperature at which a glass piece may be handled without elongating or distorting under its own weight, corresponding to a viscosity of 4×10^6 Pa-s (Littleton softening point) [ASTM C338]. For the major families of low-melting glasses, these are summarized in Table 2. Other than describing the lower temperature limit of liquid behavior, these metrics have limited value in predicting operating temperatures for vitrification processes.

To incorporate technetium at temperatures <700 °C, these four low-melting glass families may be candidate matrices. The limitation of phosphate and borate glasses are their relatively poor chemical durability, and tendencies toward phase separation and crystallization, although these characteristics may be modified with certain additives. Vanadium is a RCRA regulated element with a TCLP limit of 1.6 mg/L under the LDR Non-Wastewater Standard, not much higher than that of lead (0.8 mg/L), while phosphorus, bismuth and boron are unregulated. Little data is available on vanadate glass durability, so

it is difficult to generalize its likely performance during on-site disposal. These considerations will inform the prioritization of glasses in the following discussion.

Table 2. Typical properties of low-temperature oxide glass families [He 2016b; Appendix A and B]. RCRA Land Disposal Requirements (mg/L TCLP) for metallic elements are also provided, where applicable.

Glass Family	Transition temperature (T_g, °C)	Softening temperature (T_f, °C)	LDR Standard (mg/L)
Lead, PbO	<400	<400	0.8
Vanadate, V_2O_5	260-420	270-440	1.6
Phosphate, P_2O_5	280-500	350-600	-
Bismuthate, Bi_2O_5	360-500	430-510	-
Borate, B_2O_3	400-600	430-610	-

Two research directions in the past decade have significantly impacted this literature survey and recommendations. First, many new electronics sealing glasses have been developed in the past decade, with a particular focus on replacement of lead-based sealing glasses with "green" alternatives. Useful properties for sealing glasses include low processing temperatures and good chemical durability, characteristics that are also key for our application. In fact, one review article recognizes nuclear waste immobilization as a bulk-scale application for these low-melting glasses [Maeder, 2013]. While a great variety of compositions are available, even the lead-free formulations typically contain other elements of concern for RCRA land disposal requirements, especially zinc (4.3 mg/L TCLP limit) and vanadium (1.6 mg/L), and occasionally barium (21 mg/L) and antimony (1.15 mg/L). Leachability considerations must therefore address not only long-term technetium mobility but also release of RCRA metals above LDR standards.

Second, iodine-129 immobilization in glasses has been pursued in research for DOE Nuclear Energy programs, especially at Sandia National Laboratories and at the Korea Atomic Energy Research Institute (KAERI). The ^{129}I immobilization problem is relevant to that of ^{99}Tc, with parallels in the nuclides' long half-lives, water solubility, and volatility. Studies of glass waste forms for ^{129}I have supposed that the iodide would be captured from off-gasses as an insoluble silver salt, AgI, although other capture materials have been proposed [Riley, 2016]. Composite materials have been successfully prepared by low-temperature encapsulation of these iodine-containing materials with glass, and several will be discussed below. In general, researchers who are pursuing waste encapsulation applications for low-temperature glasses are most likely to have reported leach testing data that allows us to assess the chemical durability. As a result, there is some bias in this report toward recommending glasses that have recently been tested for radioiodine immobilization.

Appendix A summarizes the melting and sintering temperatures of several families of binary and ternary glasses, while Appendix B provides the similar information at the detailed compositional level. A number of glasses with melting temperatures as high as 800 °C are included in these summaries, because their sintering temperatures are likely to meet the threshold of <700 °C processing temperatures if used to prepare GCMs.

Low Temperature Vitrification

Preliminary Process Considerations

Many different types of electrically-heated melters have been developed and used in the vitrification of radioactive wastes. Joule heated melters (JHMs) are currently used or in development worldwide for vitrifying liquid high-level waste, and can typically process 3 metric tons per day per melter [NRC 2011]. HLW is typically processed into borosilicate glass at 1150 °C [Marra 2014], but reduced-temperature operation is also possible for a low-melting glass. The JHM operates by resistive heating, passing current between water- or air-cooled electrodes submerged in the molten glass in a refractory lined chamber. Electrode lifetime may be extended at lower operating temperatures, provided that the alternative glass formulations are not more corrosive [Gombert 2003]. With two decades of successful operating experience at the Savannah River Site, Joule-heated melter technology is the current DOE-EM baseline for waste immobilization at the Hanford site, and is a candidate technology for continuous low-temperature glass processing.

Cold crucible induction melters (CCIMs) have been used in France and Russia for years, and in bench-scale testing at the Idaho National Laboratory [Rutledge 2013, Crum 2014]. In contrast to the JHM, the CCIM employs induction heating by coupling a water-cooled high frequency electrical coil to the glass melt, causing eddy currents that heat and mix the glass. While CCIM is most recognized for trouble-free operation at higher temperatures than traditional JHM, it can also be used at the lower temperatures targeted in this report. The CCIM is smaller and less expensive to operate, and it allows for more flexible glass chemistries than JHM because it is more tolerant of crystal formation. Advanced computational fluid dynamics modeling capabilities for glass melting by CCIM have been developed for DOE-EM needs [Roach 2008]. In concert with experimentation, modeling can be used to optimize system design and to predict operational behavior for specific materials and system configurations, allowing automated feedback control. CCIMs are considered to be operationally simpler and allow for faster recoveries from system upsets than JHMs [NRC 2011], and may therefore be more suitable for discontinuous processing of small quantities of a technetium secondary waste stream over decades of planned Hanford site remediation.

All three candidate waste streams are potentially suitable for low-temperature vitrification, although process-scale vitrification of an organic ion exchange resin is unprecedented. Relatively few oxide glasses have documented melting temperatures below 700 °C, but others might be identified if a screening campaign of low-temperature glasses listed in Appendix B was undertaken. Feeds containing sodium pertechnetate, either absorbed on a non-elutable polystyrene-based resin (Purolite A530E) or as an aqueous stream from hot-water elution of Superlig-639, may benefit from the presence of a reducing melt composition, or from a reducing or inert processing atmosphere. Resin beads may provide a sufficiently reducing environment to assist in immobilizing the technetium during melting and disposal, but their effects on the glass forming process (metal reduction, off-gassing, flammability, emissions) and product stability must be evaluated. Vitrification of a solid Tc(IV) oxide feed is also feasible, but if atmosphere is not controlled, there is a risk of oxidizing the Tc to its more mobile pertechnetate form.

Candidate Glasses

Lead borate (**Pb-B**) glasses have extraordinarily low melting temperatures, ranging from 545 °C for the nominal 40 mol% PbO glass, down to 465 °C for the nominal 70-80 mol% PbO formulations [Erdogan 2014].[†] These glasses have been examined for their potential as waste forms for radioactive cesium and strontium wastes. Chemical durability of glass monoliths was tested under MCC-1 conditions (90 °C for 7 days in DI water) for the binary oxide glasses, and for selected glasses loaded with 20-30 mol% SrO or CsO. All of the waste glass samples were prepared at 950-1050 °C for these high radionuclide loadings, so the true melting points of the Sr- and Cs-containing glasses are currently unknown. However, it is possible that lower processing temperatures can be used to load the glasses with ^{99}Tc that is introduced as a sodium-bearing aqueous eluent solution or as a slurry of non-elutable ion exchange resin.

The high-lead content glasses were the lowest melting and the most chemically durable, losing overall mass in the MCC-1 test at an average rate of <1 g/m^2/day during the time period 24-174 hours. When loaded with Cs_2O (20-25 mol%) or SrO (20-30 mol%), the waste forms leached Pb at rates between 10^{-3}-10^{-2} g/m^2/day, and boron at 0.1-10 g/m^2/day. Not surprisingly, the glasses loaded with large amounts of alkali metal (Cs) were less durable than their Sr-containing analogues. Loaded analogously with 5-20% $NaTcO_4$, it is very plausible that these glasses could pass the LDR standard for Pb release. Lead borate binary glass may also be a suitable candidate for encapsulating TcO_2/Sn/Cr in a glass composite material, but there is no particular advantage over the bismuthate materials that are discussed in the next section. Experimentation on this system should begin with assessing whether the lead borate systems (70-80% Pb) melt below 700 °C with addition of waste surrogates containing $NaReO_4$ or ReO_2, and subsequently whether the products have chemical durability comparable to the host glass. Lead borate glasses may also be unstable with respect to devitrification [Bajaj 2012], so phase stability needs to be characterized.

Certain lead tin fluorophosphate (**Pb-Sn-P-O-F**) glasses also melt at ultra-low temperatures (<450 °C) and have very good chemical resistance to water attack [Tick 1984]. Abbreviated as **Pb-Sn-P** elsewhere in this report, the glasses are prepared from SnF_2–PbF_2–SnO–NH_4HPO_4 mixtures. Good waste form candidates are the glasses with mol% composition 59% Sn, 6.4% Pb, and 34.0 % P, and with 57% Sn, 6.2% Pb, and 37% P (O and F content is detailed in Appendix B). In an ad-hoc durability measurement, these glasses lost only 0.01-0.1 g/m^2/day of their total mass after 24h at 50 °C. To place this on a comparative basis with standard leach test procedures at 90 °C, we can approximate that the rate of dissolution doubles with every 10 °C temperature increase [Pauling 1988]. Even at 16 times the observed 50 °C dissolution rate, the parent glasses appear to have good durability as potential waste forms. However, this durability exists within a fairly narrow range of compositions. When the Sn content was raised or lowered by 10-20%, the leach rate increased by several orders of magnitude. This complex behavior makes its use as a technetium waste form technically risky. Also, some release of fluoride

[†]One reviewer challenged the reported melt temperatures for these glasses, postulating that the glass is phase-separated and the second endotherm, attributed to melting, is actually the glass transition temperature associated with the second phase.

occurs when this glass is prepared, which could add complexity to off-gas management and control of final glass composition.

Sodium aluminum phosphate (**Na-Al-P**) glasses have been evaluated for waste encapsulation at the United Kingdom's Atomic Weapons Establishment [Donald 2006]. The nominal composition 40 mol% Na_2O, 20% Al_2O_3 and 40% P_2O_5 was modified by adding up to 10 mol% Fe_2O_3 or B_2O_3. Compared to the nominal Na-Al-P glass, which melts at 741 °C, addition of Fe_2O_3 tended to raise the melting temperature and improve the durability, while addition of B_2O_3 at 10 mol% reduced the melting temperature to 690 °C. The durability of the Na-Al-P-B glasses was tested by measuring total mass loss after 28 days at 70 °C in DI water. As a crude estimate, this treatment may produce a similar overall effect as the 20 °C higher temperature and one-fourth duration PCT-A test. Mass losses were <0.5% for the higher-melting Fe glasses, but as much as 2-5% for the B glasses. Further evaluation of this category of glasses may be merited, based on the absence of RCRA-listed components, but improvements in durability and melting temperature are needed.

Low Temperature Glass-Ceramic Materials

Preliminary Process Considerations

Unlike vitrification, which achieves complete dissolution of the waste in its host glass, a GCM encapsulates distinct and identifiable particles of the waste within a network of glass that has been made to flow and seal around it. A potential advantage of the GCM approach is that the composition of the host glass, and consequently its processing temperature, is not significantly altered by mixing with the waste material. This feature is especially useful for addressing the low-temperature processing objective for a technetium secondary waste stream. Waste loadings of 20-25% are typical in research publications on iodide encapsulation, which are described below [Mowry 2015, Garino 2011]. There are a large number of glasses in Appendix B with reported sintering temperatures below 700 °C, and an even greater number that have softening points in the 400-500 °C range, a good indicator of their potential to be used in GCMs for technetium. Many are lead-free, although most contain other elements such as zinc that are subject to RCRA LDR limits. Modification of GCM formulations with divalent tin (*e.g.*, SnO) to provide extra stability to technetium during long-term storage may also be possible.

Cold uniaxial pressing followed by sintering, and hot pressing (uniaxial or isostatic) approaches have been used to fabricate composite nuclear waste forms in the laboratory and at larger scale, *e.g.* Synroc type and glass composite materials [Ringwood 1981]. Large-scale monoliths up to tens of kilograms in mass can be formed by pressing, meeting the throughput and scale requirements for a technetium waste form, but cracking must be controlled. Different fabrication techniques may produce different density, particle size, and phase separation characteristics in the product, all of which may affect the chemical and mechanical durability. Off-gassing from an aqueous solution or slurry is a particular issue for pressed waste forms. Even in case of a slurry of precipitated TcO_2/Sn/Cr, it may be necessary to pre-calcine or pretreat the waste to a dry oxide form to avoid shrinkage during processing. Other issues including thermal physical properties (e.g., thermal expansion and conductivity) and mechanical properties (e.g., hardness, toughness, etc.) should also be considered to minimize physical degradation.

Candidate Glasses

Bismuthate glass

Bismuthate glasses such as **Bi-Si-Zn** and **Bi-B-Zn** oxide glasses are useful candidates for immobilization of precipitated TcO_2/Sn/Cr into a glass composite material. Ferro and 3M Corporations sell a variety of low temperature bismuthate glasses for hermetic sealing, encapsulation and coating of metal, ceramic and glass substrates and components, and for use as binding agents for metal and ceramic pastes. The peak firing temperatures, a typical temperature to melt the powder into a glass, are lower than 600°C (Appendix B).

Bismuthates have a good track record in bench-scale testing to date. For example, researchers at Sandia National Laboratories have shown that GCM waste forms are easily synthesized and yield durable monoliths that retain iodine during sintering and during leach testing [Garino 2011; Mowry 2015]. For ^{129}I encapsulation, the team used a low-sintering **Bi-Si-Zn** oxide sealing glass purchased from Ferro (EG2922; 63.4 wt% Bi_2O_3, 23.4% SiO_2, 7.8% ZnO and 5.4% Al_2O_3). Silver iodide particulates (AgI or AgI-Mordenite) were blended in a 25:75 ratio with Bi-Si-Zn oxide glass powder, dry pressed and sintered at 550°C for 1 hour in air. The resulting composite material could be further isolated from environmental exposure by incorporating it into integrated core/shell structures (Figure 1), using a shell material that is well-matched to the coefficient of thermal expansion of the core to prevent cracking.

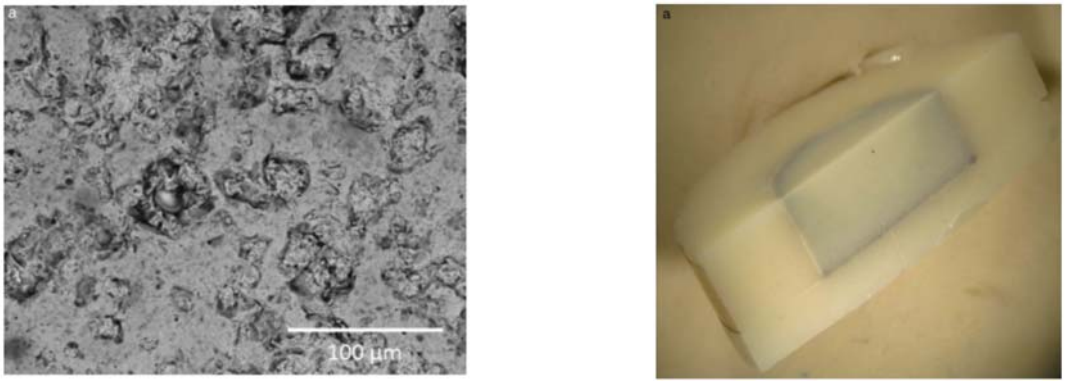

Figure 1. Glass-composite material prepared by sintering a Bi-Si-Zn glass with silver iodide (AgI) powders. Left: scanning electron microscopy image of the sintered mixture. Right: optical image of a sintered core/shell sample, where the core is glass-AgI composite and the shell is glass. [Garino 2011].

The EG2922 Bi-Si-Zn oxide glass dissolves at a very slow rate and limits the release of iodine from the embedded AgI particulates. Durability testing has been performed using both static (PCT-B, MCC-1) and dynamic (SPFT) methods, over a range of variables including pH and waste loading. In the PCT-B leaching test, the AgI/EG2922 composite material was reported to release B and Si at about 1/10 the rate of Pyrex borosilicate glass, while the AgI-mordenite composite was about as durable as Pyrex [Garino 2011]. Specifically, for an AgI-mordenite monolith containing 5 wt% iodide exposed to near-neutral water, the authors reported an average of 19.5 ppm of silicon in the effluent in the MCC-1 test (pH 8.2-8.3) and 53.1 ppm in the PCT-B test (pH 7.5-7.6). Using the density and surface area estimates provided in the Experimental section of the paper, the average leach rates for silicon were 0.24 g Si/m^2/day (MCC-1) and 0.081 g Si/m^2/day (PCT-B) [Mowry 2015].

Bi-B-Zn oxide glasses possess sintering and glass transition temperatures in the same range as Bi-Si-Zn glasses. The Sandia team has also prepared glass-composite materials using Ferro's EG2998 product, a Bi-Zn-B oxide sealing glass (60.7 wt% Bi_2O_3, 27.8% ZnO, and 11.3% B_2O_3), but durability testing has not been reported [Garino 2011]. Yang *et al.* at KAERI captured iodine using a Bi-based sorbent on mesoporous silica, and then encapsulated this material with low-temperature sealing glasses formulated to mimic Ferro's EG2998 and EG2922 glasses [Yang 2016]. The sintering temperature was 600 °C and compositions varied from 6 to 19% waste in the glass. The leaching rates of Si, Zn, and I from these materials were on the order of 10^{-2} g/m^2/day (PCT-B protocol), while boron was leached at ~0.5 g/m^2/day. These values are comparable to the Hanford performance specification for the major constituents of borosilicate HLW glass (0.3 g/m^2/day).

The rheological and thermal properties of the host glasses can be further altered by compositional variations. For example, Bi-B-Zn glasses with 74.7% Bi_2O_5 and 8.8% ZnO have been prepared using B_2O_3 content between 5.2 and 9.2%. The balance of the content of these glasses was Cu, Co, Ba or rare earth elements at <5% levels [Feng 2016]. These glasses have transition temperatures between 335-363 °C, and softening temperatures between 363-397 °C, significantly lower than the Ferro EG2998 material. Their chemical durability and suitability for encapsulation of particulates has not been tested, but the lower processing temperatures and reduced zinc content may make them suitable alternatives to the Ferro glasses. Numerous other electronic sealing glasses from 3M and Ferro Corporations are listed in Appendix B.

The iodide-containing particles that have been encapsulated in these glasses were 15-50 µm in diameter for the AgI, and 100-250 µm for the AgI-mordenite [Garino 2011]. The non-elutable Purolite A530E resin beads have a much larger particle size range of 300-1200 µm, according to their product data sheet. Combined with the potential off-gassing of water, ammonia and hydrocarbons, this larger particle size increases the relative technical risk of using a GCM to immobilize TcO_4^- absorbed on resin.

Phosphate glass

Phosphate glass has been proposed to host HLW in several countries, especially Russia [Ojovan 2007]. P_2O_5 is an oxide glass former that tends to enable low-temperature processing, but phosphate glasses generally also have low chemical durability (higher water absorption and leachability). The durability of phosphate glasses can be improved without significantly raising melt temperatures, by substitution of a portion of the P_2O_5 with Bi_2O_3 (<40 mol%) or ZnO [Shih 2001, Takebe 2006]. For example, the KAERI group published a study on ^{129}I waste encapsulation using **Bi-M-P (M = Zn, Ca, Mg, Na)** oxide glasses [Yang 2013]. Compositions were varied to identify the glass-forming regimes: Bi_2O_3 between 0-30 mol%, ZnO between 0-30%, and P_2O_5 <60%. Then, a nominal binary composition of 60 mol% Bi_2O_3 and 30% mol% P_2O_5 was modified with ZnO, CaO, MgO, or Na_2CO_3 for greater durability, with ingot formation around 600-650 °C.

These glasses were used to seal AgI particles at a mixing ratio of 0.25 AgI:0.75 glass. The PCT-B leaching test was used to measure chemical durability (90 °C, 7 days). While silver and bismuth did not leach appreciably in these tests (~10^{-4} g/m^2/day), significantly larger amounts of soluble phosphate (4.4-4.8 g/m^2/day) and other additives (Zn, Ca, Mg, Na; 4-7 g/m^2/day) were released. Therefore, the Bi-M-P glasses are about 16 times more leachable than the standard for borosilicate glass. Despite their limited

durability, these are among the small number of low-temperature glass formulations that contain no RCRA elements. The good performance of the sodium-containing glass suggests the possibility of encapsulating $NaTcO_4$ from a pre-dried anion exchange eluent. Furthermore, if divalent tin oxide can replace the other divalent metal oxide modifiers in this glass, the resulting GCM would provide a reducing environment in which to encapsulate TcO_4^- or TcO_2 species.

A group in Taiwan developed a series of lead-free **P-Na-Cu** oxide glasses for low-temperature applications (50 mol% P_2O_5, 20% Na_2O and 30% CuO). [Shih 2001] These glasses have low transition temperatures T_g ~290-360°C) and the authors claimed excellent chemical durability, with dissolution rates as low as 0.8 g/m^2/day at room temperature. However, a standard 90 °C test was not performed, so these values cannot be directly compared to other glasses in this report. Applying the rule of thumb that reaction rates double with each 10 °C increase in temperature, the equivalent dissolution rate for these glasses in a 90 °C test would be about 100 g/m^2/day. Despite the authors' claim of excellent durability, then, this glass family is not a priority for technetium immobilization.

Borate glass

Although B_2O_3 glasses are also low melting compared to borosilicate glasses, most borates that have been tested have unacceptably low durability to be used for nuclear waste immobilization [Bengisu 2016]. Lead borate, which was discussed above as a candidate for low-temperature vitrification, is a possible exception. In contrast to the low-borate glasses discussed above, the chemical durability of low-melting formulations of Bi-B-Zn that contain 45 wt% B_2O_3 is quite low [Liu 2012], highlighting the variations in structure and durability that can occur within the borate family.

Finally, the **B-Al-Na** glass system yields vitreous materials in the composition range >60 mol% B_2O_3, <20% Na_2O and <20% Al_2O_3. In many cases the glass transition temperatures are between 330-460 °C and softening points are between 370-500 °C [Ding 2014]. Melting temperatures have not been reported for this system. Durability also has not been reported, but if adequately high, there is the possibility of using B-Al-Na glasses to encapsulate sodium-bearing materials (i.e. TcO_4^- absorbed on A530E anion exchange resin). Because these glasses contain no RCRA elements, a preliminary study of their durability may be warranted.

Low Temperature Sol-Gel Processing

Sol-gel processing is a route to glass or mineral formation that has been occasionally examined for nuclear waste immobilization. It is perhaps the ultimate low-temperature route, because the initial glass network formation occurs during a rapid, room-temperature chemical reaction of a colloidal silica solution. Drying may require temperatures nearer 100 °C, and additional compaction may be desirable. Sol-gel processes tend to be highly tolerant of additives; for example, incorporation of salt and oxide surrogates into durable waste forms has been demonstrated in proof-of-concept experiments [Deptula 2011, Zelinski 1998]. A significant drawback, however, is the need to collect and manage hydrolysis byproducts such as ethanol or methanol. Fracturing of the glass during the drying step has also historically limited the interest in sol-gel routes for waste disposition, but recent improvements have addressed much of the fracturing issue and made dense monoliths possible [Kajihara 2013].

Incorporation of sodium nitrate solutions with moderate to high alkalinity has also been demonstrated at LANL. In a proprietary sol-gel process, the silica precursor is pretreated to obtain an activated solution, then added to aqueous solutions of variable pH. The resulting solutions will gel over time and then can be dried to form a glass at <100 °C. These studies were recently expanded to high pH, and glasses were successfully produced from solutions containing 0.5 M $NaNO_3$. The gelation times (0.5-6 min) depend on temperature, ionic strength, silica concentration, and pH and can be tuned to meet process requirements. Rapid gelation at higher temperatures and ionic strengths results in the production of powder that could be turned into a monolith with a second gelation step, or used as the feed to a low temperature encapsulation process.

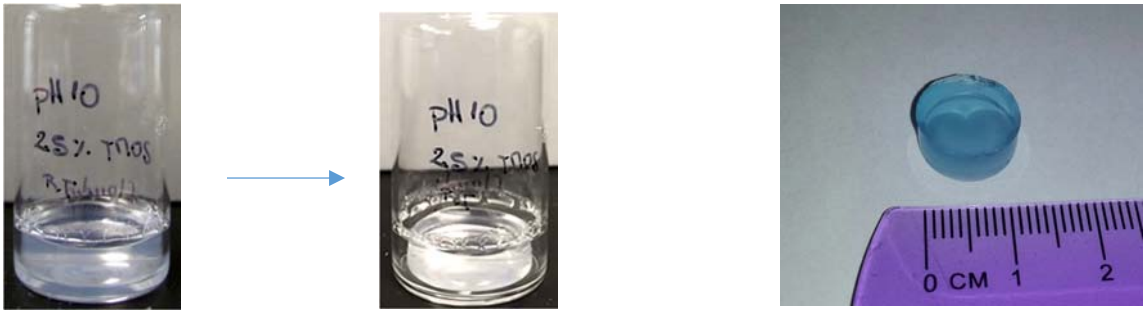

Figure 2. Examples of sol-gel processing of alkaline nitrate solutions. Left: Room-temperature gelation of a pH 10 solution is followed by 1-2 days of drying at <80 °C to form a dense glass. Right: Incorporation of 0.5 M sodium nitrate in alkaline solution also results in a dense monolith at <100 °C (blue color added to aid in visualization) [LANL, unpublished].

These initial results suggest the possibility that sol-gel processes can be used to form glass powders and monoliths to immobilize Tc-containing anion exchange eluent solution. Incorporation of salt aids in the gel formation, and the process has been initially shown to work with acid- and salt-containing feeds, such as the eluent from SL-639 resin, for direct monolith formation. The incorporation of other solids, such as the $NaTcO_4$-loaded anion exchange resin, could also be accommodated, provided the solid can be well-suspended in the sol while the gel is forming. This route could address one of the major limitations of cementation of non-elutable resins, namely that the water within the resin releases and degrades the cement over time [Valenta 2010]. In a sol-gel process the water within the resin would be removed at the time that the gel is dried. Despite these possible advantages, questions about durability and process scale-up require us to rate sol-gel processing as a higher-risk approach than others in this report.

Summary of Literature Survey

In Table 3, properties of the candidate glasses from this literature evaluation are summarized. Each of these glasses is carried forward into thermodynamic modeling in the next section.

Table 3. Summary of literature compositions, durability data, preferred application for the possible Tc waste streams, and potential processing temperatures[‡], for selected candidate glasses.

Tested Glass	Glass Composition	Durability Test Results ($g/m^2/day$)	Applicable Tc Stream	Process Temp. (°C)	References
Pb-B	80 PbO, 20 B_2O_3 (mol%) Blended with up to 30% SrO, or 65 PbO, 35 B_2O_3 (mol%) Blended with up to 30% Cs_2O	**Static** MCC-1 test, 7 days, 90 °C <1 (overall mass, Pb-B only); 10^{-3}-10^{-2} (Pb, from Cs/Sr loaded glass); 0.1-10 (B, from Cs/Sr loaded glass)	Ion exchange eluate (TcO_4^-)	460-470 Melt[‡]	Erdogan 2014
Sn-Pb-P-O-F	59 Sn, 6.4 Pb , 34.0 P (mol%) 60.4% F 121.5% O (per cation)	**Static** Leach test, 24 h, 50 °C 10^{-2}-10^{-1} (overall mass)	Ion exchange eluate (TcO_4^-)	450 Melt[‡]	Tick 1984
Bi-Si-Zn (EG 2922)	63.4 Bi_2O_3, 23.4 SiO_2, 7.8 ZnO, 5.4 Al_2O_3 (wt%) Blended with ≤10% AgI-Mordenite	**Static** MCC-1 test, 7 days, 90 °C 0.24 (Si) PCT-B test, 7 days, 90 °C 0.081 (Si) **Dynamic** SPFT at 25 °C 10^{-3} (Zn), 10^{-4} (Si)	TcO_2/Sn/Cr precipitate	<600 Sinter	Mowry 2015, Garino 2011
Bi-B-Zn (EG 2998)	60.7 Bi_2O_3, 27.8 ZnO , 11.3 B_2O_3 (wt%) Blended with ≤25% Bi_2O_3 and up to 19% Bi-SBA-I	**Static** PCT-B test, 7 days, 90 °C 10^{-2} (Si, Zn), 0.5 (B)	TcO_2/Sn/Cr precipitate	600 Sinter	Yang 2016, Garino 2011
Bi-Ca-P *or* Bi-Na-P	60 Bi_2O_3, 30 P_2O_5, 10 CaO or 60 Bi_2O_3, 30 P_2O_5, 10 Na_2O (mol%) Blended with 25% AgI waste form	**Static** PCT-B test, 7 days, 90 °C <10^{-4} (Bi), 4-6 (P, Na, Ca)	TcO_2/Sn/Cr precipitate	600-650 Sinter	Yang 2013

[‡] Reported melting temperature for parent glasses. Higher temperatures will be required for a vitrification process, to lower the viscosity sufficiently for mixing and pouring. Addition of waste stream is also expected to increase the melting temperatures.

Thermodynamic Modeling of Technetium Retention

Geochemical Modeling Overview

The short-term dissolution rates of six promising glasses, as reported in the literature, have been summarized in Table 3. These results provided an initial estimate of the expected performance of each glass for retaining technetium during on-site disposal. It is also useful to understand the long-term fate of technetium, in contact with environmental water and air, as the dissolution of the glass proceeds to thermodynamic equilibrium. To show the effects of dissolution of the different glasses, modeling was performed on the candidate glasses presented in Table 3. The approach used was similar to the modeling reported by Pacific Northwest National Laboratory for Immobilized Low Activity Waste [Pierce 2011]. The accuracy of these model results is limited by the quality of experimental data that currently exists for the key species in these novel glass waste forms. In particular, there is limited thermodynamic data available for bismuth- and technetium-containing minerals, and the glasses and waste forms must be modeled as their constituent mineral oxides/fluorides, rather than in their blended states. Chemical bonding effects between technetium and the glass, for example, cannot be treated by the current model input data.

Geochemist's Workbench (GWB), Version 11.0 was used to simulate secondary solid phase formation during candidate glass dissolution, and to determine concentrations of key species liberated into solution from these glass waste forms. Figure 3 presents the overall modeling approach used in this study. Thermodynamic databases available in Geochemist's Workbench were updated to include species and minerals that are relevant to the study. In particular, Appendix C lists the thermodynamic datasets for technetium and bismuth used for the geochemical modeling for this report [Rard 1999, Rard 2011, Minteq 2006, Norman 1998, Yang 2016]. To confirm that Geochemist's Workbench was capable of determining secondary phase formation during glass dissolution, a validation and verification exercise was completed using the experimental data from literature to compare the modeling results.

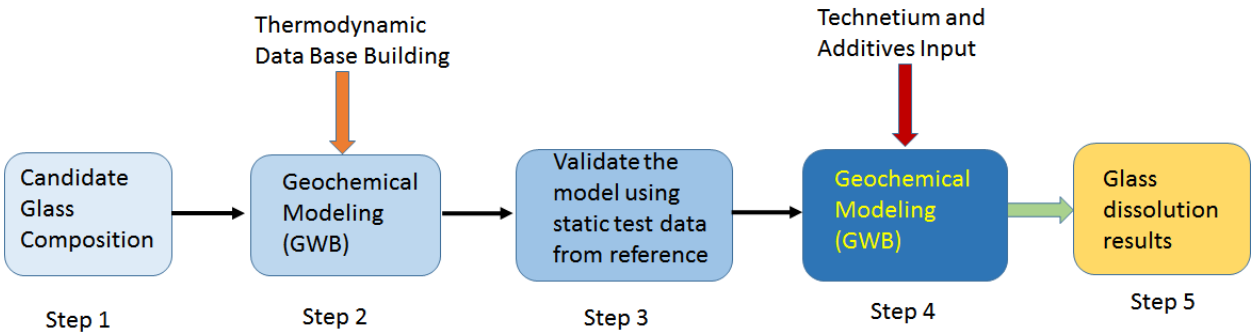

Figure 3. Schematic representation of glass dissolution geochemical modeling processes.

To determine the secondary phases that formed during dissolution of a particular glass sample, the React Module of GWB is used to trace a reaction path that takes place as a particular sample of glass dissolves in water. To set up the model, the composition of the initial fluid (near-neutral water) and the

glass composition are set and placed as input files. As the model runs, GWB assumes a certain quantity of glass dissolves into solution and system equilibrium is re-established, until the reaction progress equals 1.00, representing complete dissolution. As the reaction progresses, some secondary minerals precipitate as an altered layer while other elements are released into solution. The output files include the secondary mineral formation as the reaction progress, and solution concentrations of key species as a function of mass reacted of the original glass/waste form. The input file is also set up so that the solution in which the glass dissolves is in equilibrium with air (fO_2=0.21). The model accounts for all aqueous species that could form, redox reactions that could occur, and mineral species that could precipitate at equilibrium, based on the thermodynamic database that is used.

This modeling approach has some key limitations. As noted previously, the accuracy of the model is limited by the available thermochemical data. Geochemist's Workbench models a system that is continuously re-establishing equilibrium, and it does not take into account that elements in glasses may dissolve incongruently. For example, the heterogeneous phases in a phase-separated glass or a glass-composite material may not weather at the same rate. Furthermore, the model cannot provide any comparative rate (kinetic) data for weathering of different glasses, nor for rates of weathering *versus* precipitation of secondary minerals. Finally, the system is assumed to be in continuous equilibrium with dissolved oxygen. This implies that the source of oxygen is unlimited, and present in the subsurface at the same level as for surface water. This approach may exaggerate the availability of oxygen during on-site disposal. However, it is the most conservative assumption for evaluating the amount of divalent tin additive that would permanently stabilize technetium in the waste form.

Given these limitations, it is important to point out the benefits of the thermodynamic modeling. First, modeling can identify compositions that are thermodynamically resistant to dissolution. Such materials will, by definition, be stable in both short term (laboratory testing) and long term (on-site disposal) exposure. Additionally, the modeling can assist in designing compositions with enhanced stability, such as technetium waste forms stabilized against oxidation using stannous ion.

The following pages present modeling results for three phases of this study. First, the model validation results for two candidate glasses are presented, to demonstrate that the method and the thermochemical inputs for key species yield the correction solution species, in at least grossly accurate proportions compared to the short-term leaching studies. These two glasses were selected because good quality short-term leach test data, spanning multiple elements of interest. (i.e., Bi, Pb, Si, Zn, B), was available in the literature. Next, we present thermodynamic simulations of the complete dissolution of a $TcO_2 \cdot 2H_2O$-containing waste form based on each of the six candidate glasses. This simulation is not predictive of the *rate* of technetium release in on-site disposal, but only of the ultimate *extent*. In the third set of simulations, varying amounts of divalent tin (SnO or SnF_2) are added in an attempt to immobilize TcO_4^- in its reduced form, $TcO_2 \cdot 2H_2O$.

Geochemical Modeling Results

Model Validation for Candidate Glasses

Validation case 1: Bi-Si-Zn (EG 2922) Glass-Ceramic Material with AgI-Mordenite

- Input glass composition (wt%): 75 base material (EG 2922), 15 mordenite, 4.3 Ag, and 5 I.
- Reaction condition: 1 g of glass reacts with 10 ml DI water at near neutral pH
- Model validation: Compare to static durability test results from literature

This first validation study examines the release of key elements from the GCM prepared from an AgI-mordenite composite blended and sintered with EG 2922 glass [Mowry 2015]. Results of the modeling are presented in terms of the secondary phases calculated to form as a function of reaction progress (100 g glass/L) (Figure 4a) and the measured solution concentrations (µg/L). The measured compositions of the leachate from the PCT tests, versus model results for selected elements as a function of mass reacted, are plotted in Figure 4b. The model correctly predicts release of Bi^{3+}, Ag^{+}, and I^{-} species, and the relative proportions of these species are qualitatively comparable to experimental data.

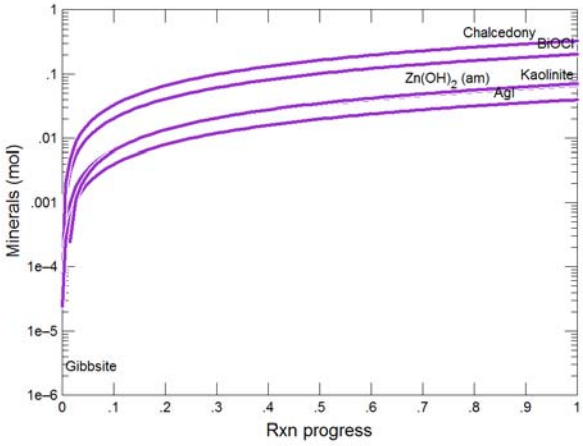

Figure 4a. Secondary phases predicted to form as a function of reaction progress (100 g glass/L).

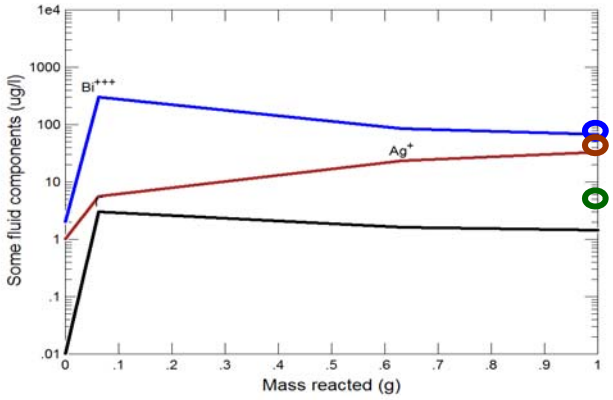

Figure 4b. Measured solution concentration (open circle) and model results (solid line) for Bi, Ag and I as a function of mass reacted.

Validation case 2: Pb-B Glass in Varying Compositions

- Input glass composition (mol%): 30 $PbO/70\ B_2O_3$; 50 $PbO/50\ B_2O_3$; 80 $PbO/20\ B_2O_3$
- Reaction condition: 1 mol of glass reacts with 1000 ml DI water at near neutral pH
- Model validation: compare to static durability test results [Erdogan 2014]

This validation case examines the release of Pb and B species from varying compositions of $PbO\text{-}B_2O_3$ glass. The model results of solution concentrations (µg/L) of as a function of mass reacted for three glasses with various compositions are presented in Figure 5a. The measured compositions of the solutions contacting the glass in the MCC-1 tests are compared to the model results for the major elements for various glass composition (Figure 5b). The model correctly predicts diminishing releases of Pb (blue data in Fig. 5b) and B (red data) with increased lead content in the glass. Those close agreement between short-term (measured) and long-term (predicted) leaching behavior may indicate that the leaching rate is thermodynamically controlled.

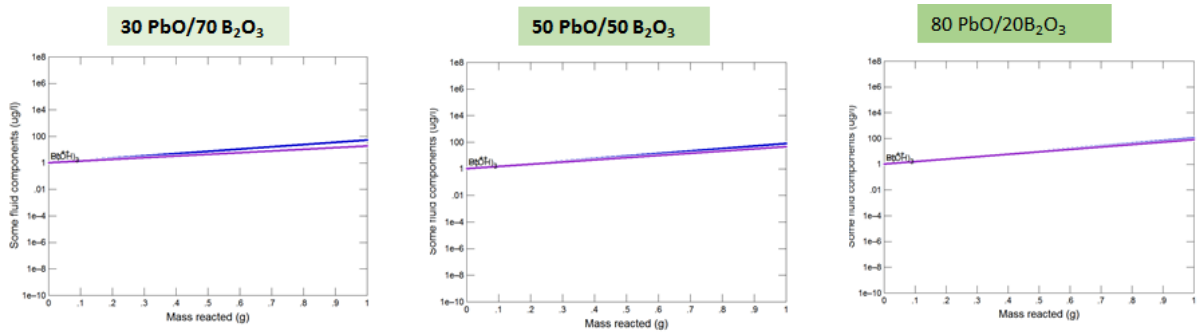

Figure 5a. Solution concentrations calculated for $B(OH)_3$ (blue) and Pb (purple) as a function of mass reacted for various composition of Pb-B glass .

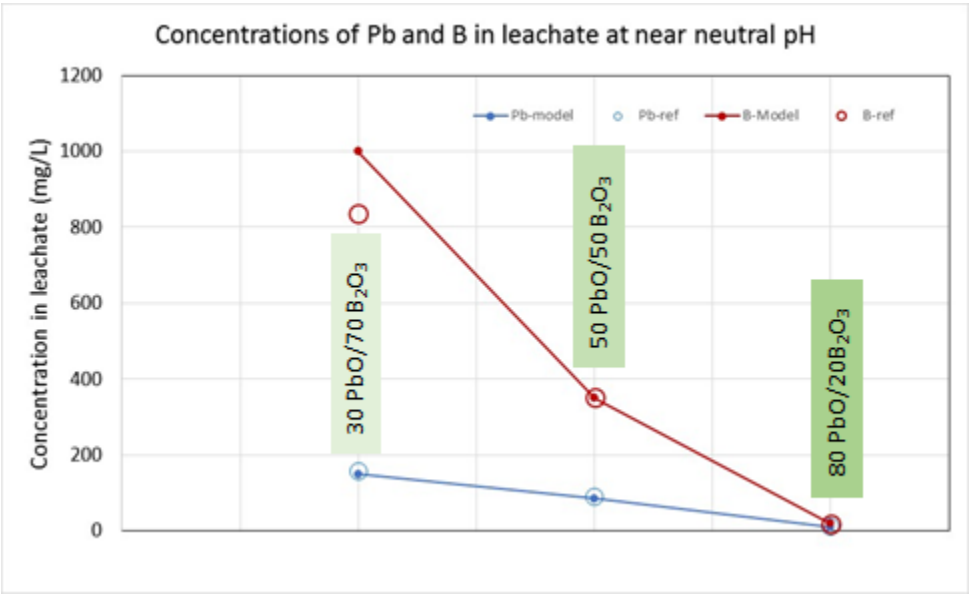

Figure 5b. Measured solution concentration (open circle) and model results (solid line) of B and Pb as function of glass composition.

Six Candidate Glasses with Technetium ($TcO_2 \cdot 2H_2O$) Added

Because of the high solubility of pertechnetate ion, thermodynamic modeling will always result in complete release unless a reducing agent is present. Instead, the objective of this section is to predict the equilibrium reactivity of waste forms containing the Tc(IV) hydrous oxide, introduced to various waste forms either as a slurry of the precipitated solid or converted via a reducing melt. No attempt is made here to model the other constituents of the waste stream, e.g. Na or Sn/Cr.

Bi-Si-Zn (EG2922) Glass + $TcO_2 \cdot 2H_2O$

- Input glass composition: (wt%) 95 base material (EG2922), 5 $TcO_2 \cdot 2H_2O$
- Reaction condition: 1 g of glass reacts with 10 ml DI water at near neutral pH

Results of the modeling are presented in terms of the secondary phases calculated to form as a function of reaction progress (100 g glass/L) (Figure 6a) and model results for selected elements as a function of mass reacted (Figure 6b). Tc(IV) is oxidized to Tc(VII) by dissolved O_2 in the solution. No TcO_4^- attenuation was observed, except for a small quantity of amorphous $TcO_2 \cdot H_2O$ secondary phase.

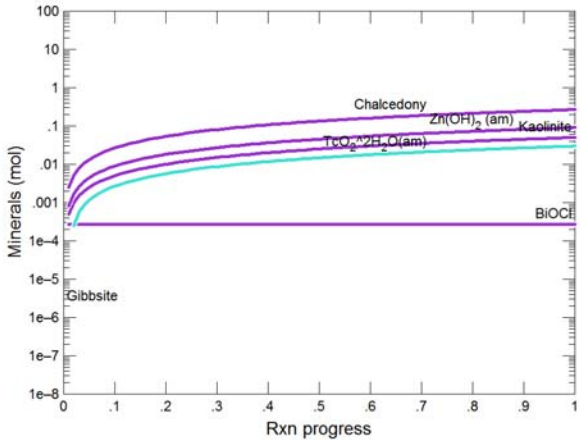

Figure 6a. Secondary phases predicted to form as a function of reaction progress (100 g glass/L).

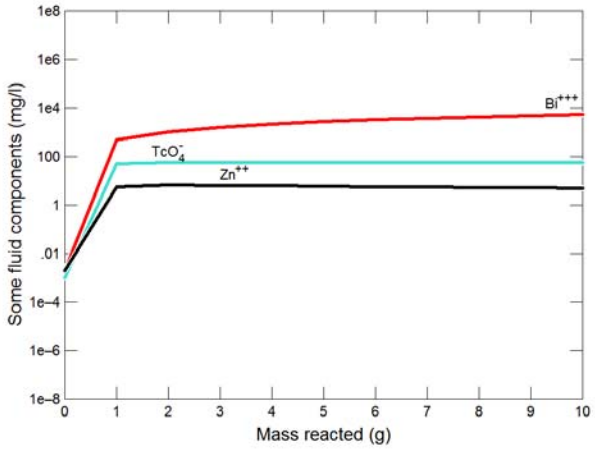

Figure 6b. Solution concentration for TcO_4^- (light blue), Zn (black), and Bi^{3+} (red) as a function of mass reacted.

Bi-B-Zn (EG2998) Glass + $TcO_2 \cdot 2H_2O$

- Input glass composition (wt%): 75 base material (EG2998), 5 $TcO_2 \cdot 2H_2O$
- Reaction condition: 1 g of glass reacts with 10 ml DI water at near neutral pH

Results of the modeling are presented in terms of the secondary phases calculated to form as a function of reaction progress (100 g glass/L) (Figure 7a) and model results for selected elements as a function of mass reacted (Figure 7b). Again, Tc(IV) is oxidized to Tc(VII) by dissolved O_2 in the solution. No TcO_4^- attenuation was observed, except for a small quantity of amorphous $TcO_2 \cdot H_2O$ secondary phase.

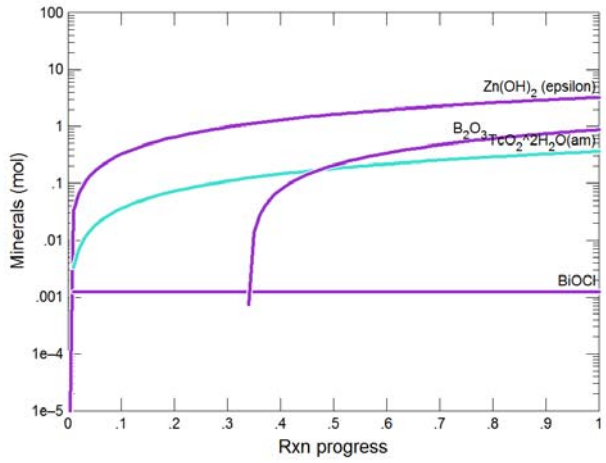

Figure 7a. Secondary phases predicted to form as a function of reaction progress (100 g glass/L).

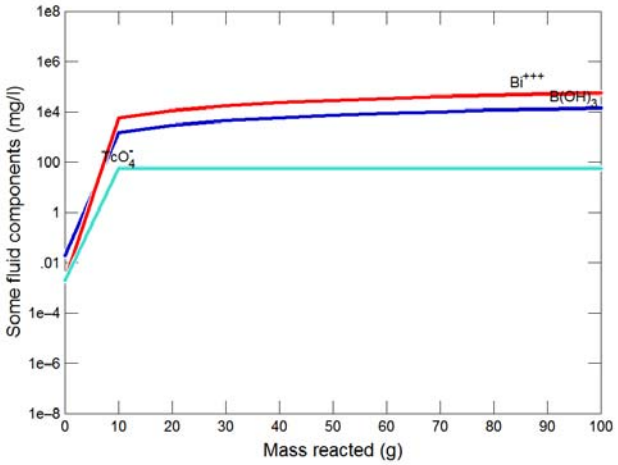

Figure 7b. Solution concentration for TcO_4^- (light blue), $B(OH)_3$ (dark blue) and Bi^{3+} (red) as a function of mass reacted.

Bi-Na-P + $TcO_2 \cdot 2H_2O$

- Input glass composition (mol%): 75 base material (Bi-Na-P), 25 $TcO_2 \cdot 2H_2O$
- Reaction condition: 1 mol of glass reacts with 1000 ml DI water at near neutral pH

Results of the modeling are presented in terms of the secondary phases calculated to form as a function of reaction progress (1mol glass/L) (Figure 8a) and model results for selected elements as a function of mass reacted (Figure 8b). Again, Tc(IV) is oxidized to Tc(VII) by dissolved O_2 in the solution. No TcO_4^- attenuation was observed, except for a small quantity of amorphous $TcO_2 \cdot H_2O$ secondary phase.

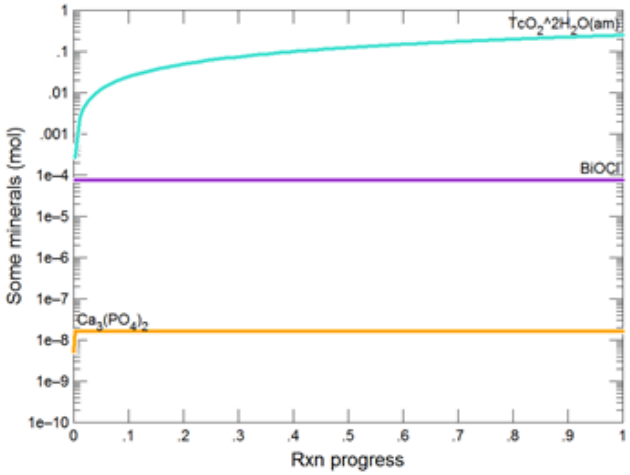

Figure 8a. Secondary phases calculated to form as a function of reaction progress (1 mol glass/L).

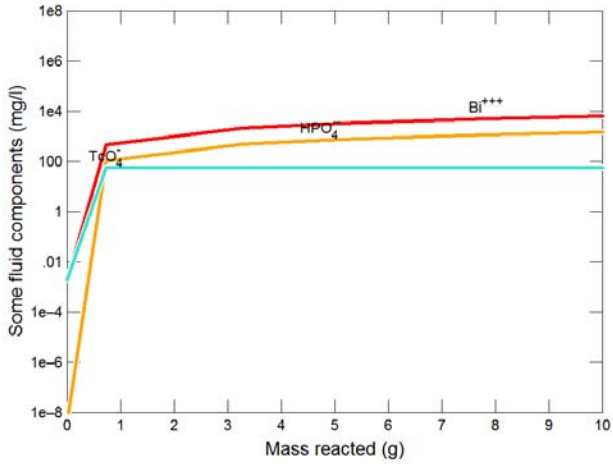

Figure 8b. Solution concentration for TcO_4^- (light blue), HPO_4^{2-} (orange) and Bi^{3+} (red) as a function of mass reacted.

Bi-Ca-P + $TcO_2 \cdot 2H_2O$

- Input glass composition (mol%): 75 base material (Bi-Ca-P), 25 $TcO_2 \cdot 2H_2O$
- Reaction condition: 1 mol of glass reacts with 1000 ml DI water at near neutral pH

Results of the modeling are presented in terms of the secondary phases calculated to form as a function of reaction progress (1 mol glass/L) (Figure 9a) and the model results for solution concentrations (mg/L, as a function of mass reacted (Figure 9b). Again, Tc(IV) is oxidized to Tc(VII) by dissolved O_2 in the solution. No TcO_4^- attenuation was observed, except for a small quantity of amorphous $TcO_2 \cdot H_2O$ secondary phase.

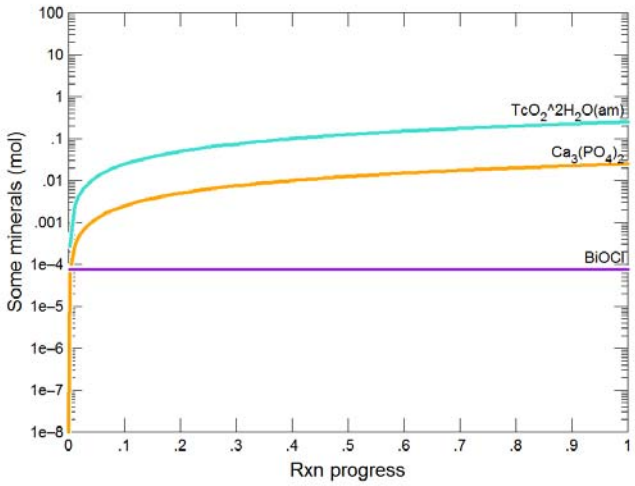

Figure 9a. Secondary phases calculated to form as a function of reaction progress (1 mol glass/L).

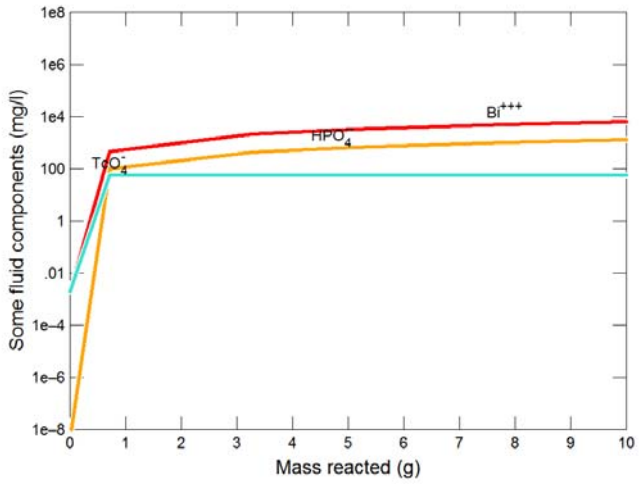

Figure 9b. Solution concentration for TcO_4^- (light blue), HPO_4^{2-} (orange) and Bi^{3+} (red) as a function of mass reacted.

Pb-B + $TcO_2 \cdot 2H_2O$

- Input glass composition (mol%): 75 [50 PbO/50 B_2O_3], 25 $TcO_2 \cdot 2H_2O$
- Reaction condition: 1 mol of glass reacts with 1000 ml DI water at near neutral pH

Results of the modeling are presented in terms of the secondary phases calculated to form as a function of reaction progress (1 mol glass/L) (Figure 10a) and the model results for solution concentrations (mg/L, as a function of mass reacted (Figure 10b). Again, Tc(IV) is oxidized to Tc(VII) by dissolved O_2 in the solution. No TcO_4^- attenuation was observed, except for a small quantity of amorphous $TcO_2 \cdot H_2O$ secondary phase. Lead is also dissolved.

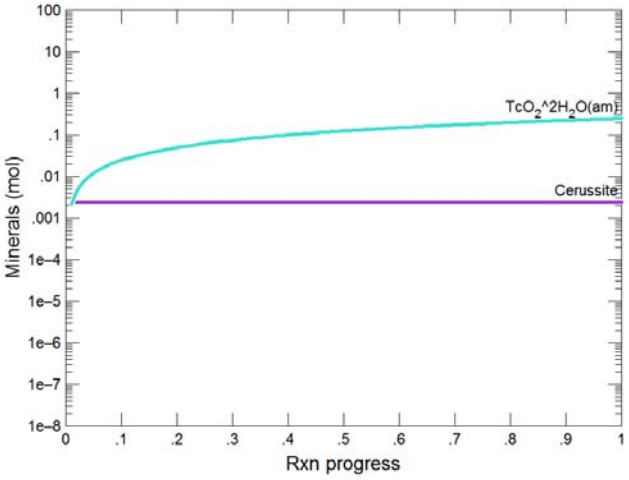

Figure 10a. Secondary phases calculated to form as a function of reaction progress (1 mol glass/L). Cerussite is lead carbonate.

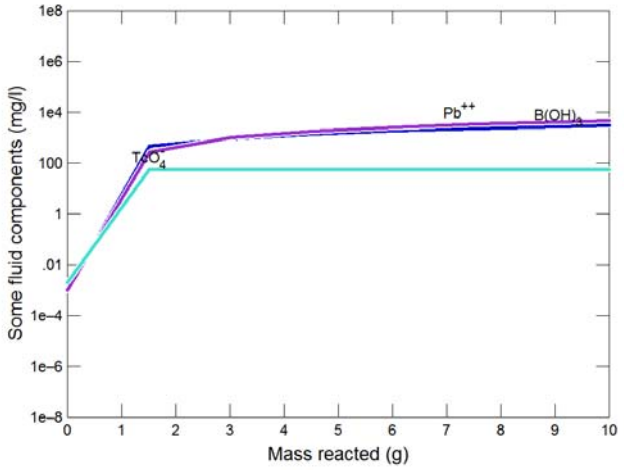

Figure 10b. Solution concentration for TcO_4^- (light blue), $B(OH)_3$ (dark blue) and Pb^{2+} (purple) as a function of mass reacted.

Sn-Pb-P+ $TcO_2 \cdot 2H_2O$

- Input glass composition (mol%): 56 SnO, 6.1 PbO, 32 P_2O_5, 5 $TcO_2 \cdot 2H_2O$
- Reaction condition: 1 mol of glass reacts with 1000 ml DI water at near neutral pH

Results of the modeling are presented in terms of the secondary phases calculated to form as a function of reaction progress (1 mol glass/L) (Figure 11a) and model results for selected elements as a function of mass reacted (Figure 11b).

In this scenario, technetium is immobilized by Sn^{2+} at early stages of reaction. As Sn^{4+} increased in the solution, Tc(IV) is increased accordingly. However, this is the only nominal glass composition that immobilized TcO_4^-, suggesting SnO may be effective as a reducing additive for immobilizing Tc in other glass formulations.

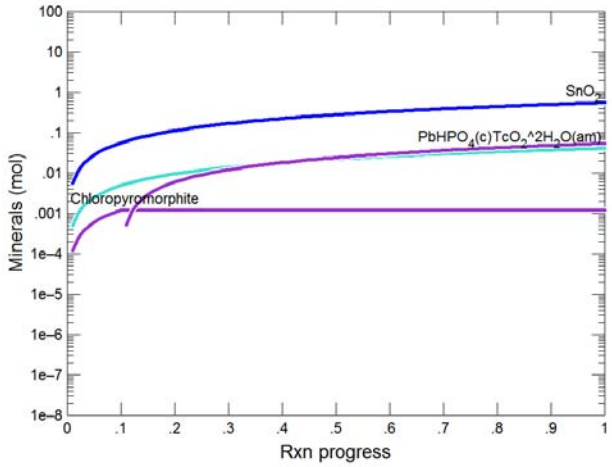

Figure 11a. Secondary phases predicted to form as a function of reaction progress (1 mol glass/L).

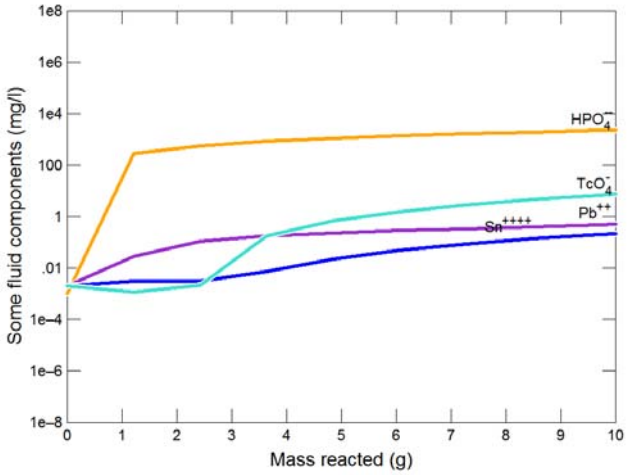

Figure 11b. Solution concentration for TcO_4^- (light blue), Sn^{4+}(dark blue), HPO_4^- (orange) and Pb^{2+} (purple) as a function of mass reacted.

Six Candidate Glasses with Technetium and Divalent Tin Added

The above results suggest that to immobilize technetium in the waste form, an additive with reducing capacity must be included in the waste form. In this study, varying amounts of SnO or SnF_2 are considered as reducing additives. This section considers both TcO_4^- and $TcO_2{\cdot}H_2O$ waste streams.

Bi-Si-Zn (EG2922) + Sn(II) + $NaTcO_4$

- Input glass composition (wt%): 75 base material (EG2922), (5, 10, 15, 20) SnF_2, 5 TcO_4^-
- Reaction condition: 1 g of glass reacts with 10 ml DI water at near neutral pH

The model results for selected elements as a function of mass reacted at various amount of SnF_2 are presented in Figure 12. The results indicate that at 3 g of SnF_2 per 1 g TcO_4^-, technetium can be immobilized. At a 2:1 mass ratio, there is insufficient reducing agent to immobilize TcO_4^-.

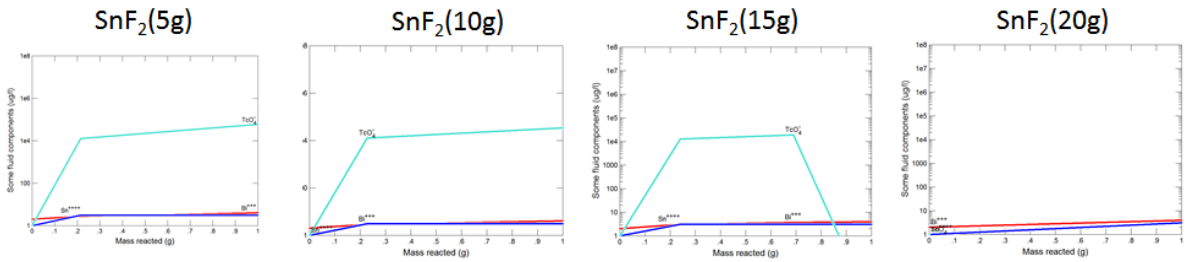

Figure 12. Solution concentration for TcO_4^- (light blue), Sn^{4+} (dark blue), Bi^{3+} (red) as a function of mass reacted at various amount of SnF_2 additive.

Bi-Si-Zn (EG2922) + Sn(II) + $TcO_2{\cdot}H_2O$

- Input glass composition (wt%): 75 base material (EG2922), (5, 10, 20) SnO, 5 $TcO_2{\cdot}2H_2O$
- Reaction condition: 1 g of glass reacts with 10 ml DI water at near neutral pH

The model results for selected elements as a function of mass reacted at various amount of SnO are presented in Figure 13. The results indicate that Tc(IV) can be oxidized by dissolved O_2 to TcO_4^-, but reduction by Sn(II) provides immobilization of the technetium at mass ratios 2:1 and greater.

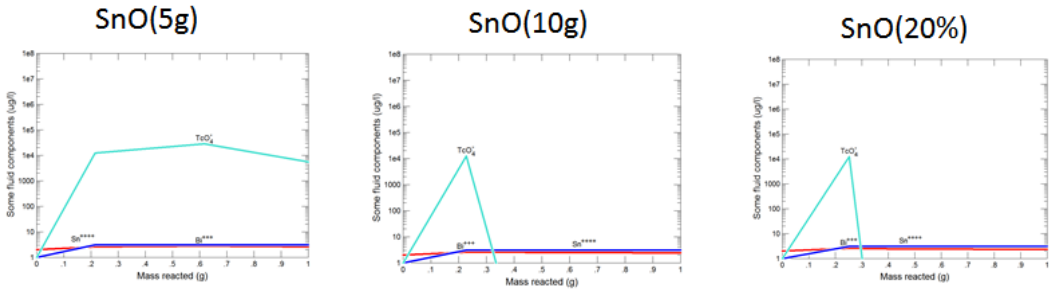

Figure 13. Solution concentration for TcO_4^- (light blue), Sn^{4+} (dark blue), Bi^{3+} (red) as a function of mass reacted at various amounts of SnO additive.

Bi-B-Zn (EG2998) + Sn(II) + $NaTcO_4$

- Input glass composition (wt%): 75 base material (EG2998), (25-x) SnO, x $NaTcO_4$
- Reaction condition: 1 g of glass reacts with 10 ml DI water at near neutral pH

Results of the modeling are presented in terms of the secondary phases calculated to form as a function of reaction progress (100 g glass/L) (Figure 14a) and model results for selected elements as a function of mass reacted (Figure 14b) at various glass composition.

Results indicate that at a ratio of 1.5 g SnO to 1 g of $NaTcO_4$, the technetium can be immobilized. At a 1:1.5 mass ratio, there is insufficient reducing agent to immobilize $NaTcO_4$.

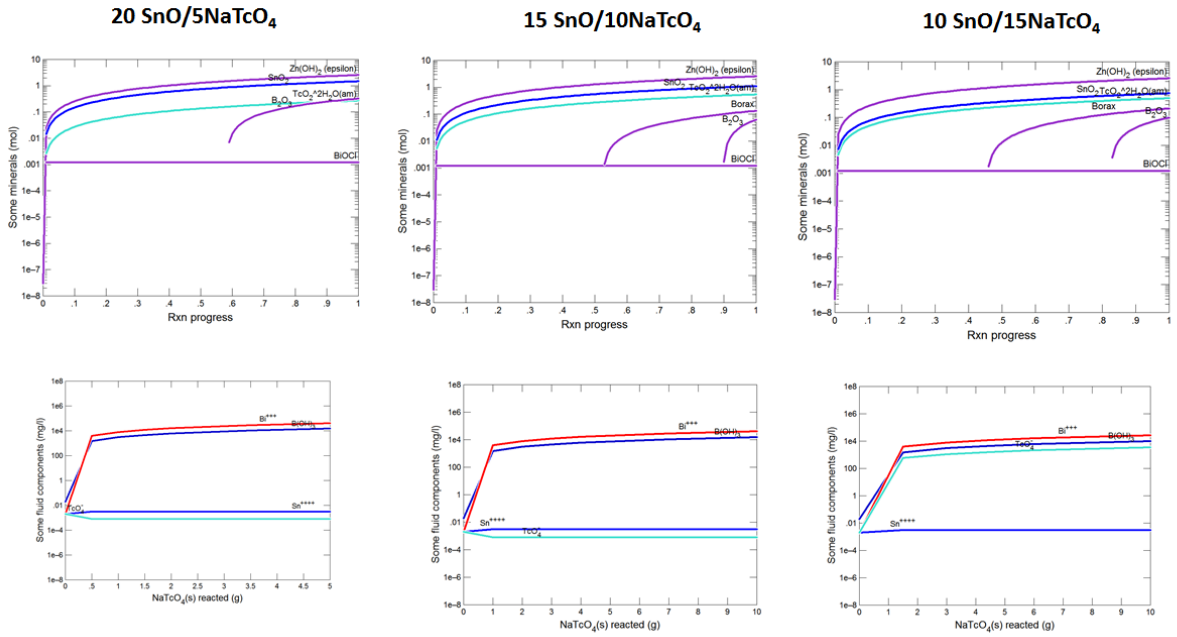

Figure 14. (a) Secondary phases predicted to form as a function of reaction progress (100 g glass/L) (top); (b) Solution concentration for TcO_4^- (light blue), Sn^{4+} (dark blue), Bi^{3+} (red), and $B(OH)_3$ (deep blue) as a function of $NaTcO_4$ reacted at various composition of glass system (bottom) .

Bi-B-Zn (EG2998) + Sn(II) + $TcO_2 \cdot H_2O$

- Input glass composition (wt%): 75 base material (EG2998), (25-x) SnO, x $TcO_2 \cdot 2H_2O$
- Reaction condition: 1 g of glass reacts with 10 ml DI water at near neutral pH

Results of the modeling are presented in terms of the secondary phases calculated to form as a function of reaction progress (100 g glass/L) (Figure 15a) and model results for selected elements as a function of mass reacted (Figure 15b) at various glass composition.

Results indicate that at 1 g SnO and above, there is sufficient reducing agent to immobilize 24 g $TcO_2 \cdot 2H_2O$. The result also indicate at 1 g SnO, Tc(IV) was oxidized first by O_2 to TcO_4^-, then reduced and immobilized.

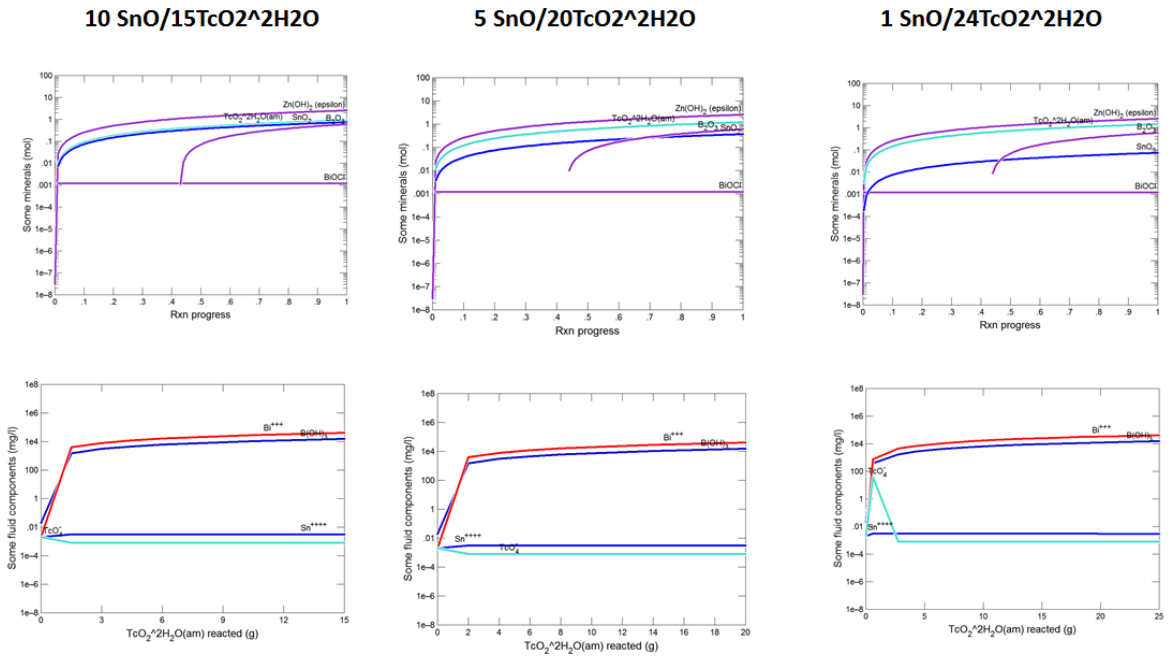

Figure 15. (a) Secondary phases predicted to form as a function of reaction progress (100 g glass/L) (top); (b) Solution concentration for TcO_4^- (light blue), Sn^{4+} (dark blue), Bi^{3+} (red), and $B(OH)_3$ (deep blue) as a function of $TcO_2 \cdot 2H_2O$ reacted at various composition of glass system (bottom).

Bi-Na-P + Sn(II) + $NaTcO_4$

- Input glass composition (mol%): 75 base material (Bi-Na-P), (25-x) Sn^{2+}, x TcO_4^-
- Reaction condition: 1 mol of glass reacts with 1000 ml DI water at near neutral pH

Results of the modeling are presented in terms of the secondary phases calculated to form as a function of reaction progress (1 mol glass/L) (Figure 16a) and model results for selected elements as a function of mass reacted (Figure 16b).

Results indicate that at 15 mol% Sn^{2+}, there is insufficient reducing agent to immobilize 10 mol% TcO_4^-. At 17.5 mol% Sn^{2+} and above, 7.5 mol% TcO_4^- can be immobilized. The corresponding mole ratios are expected to immobilize technetium at lower levels in the glass.

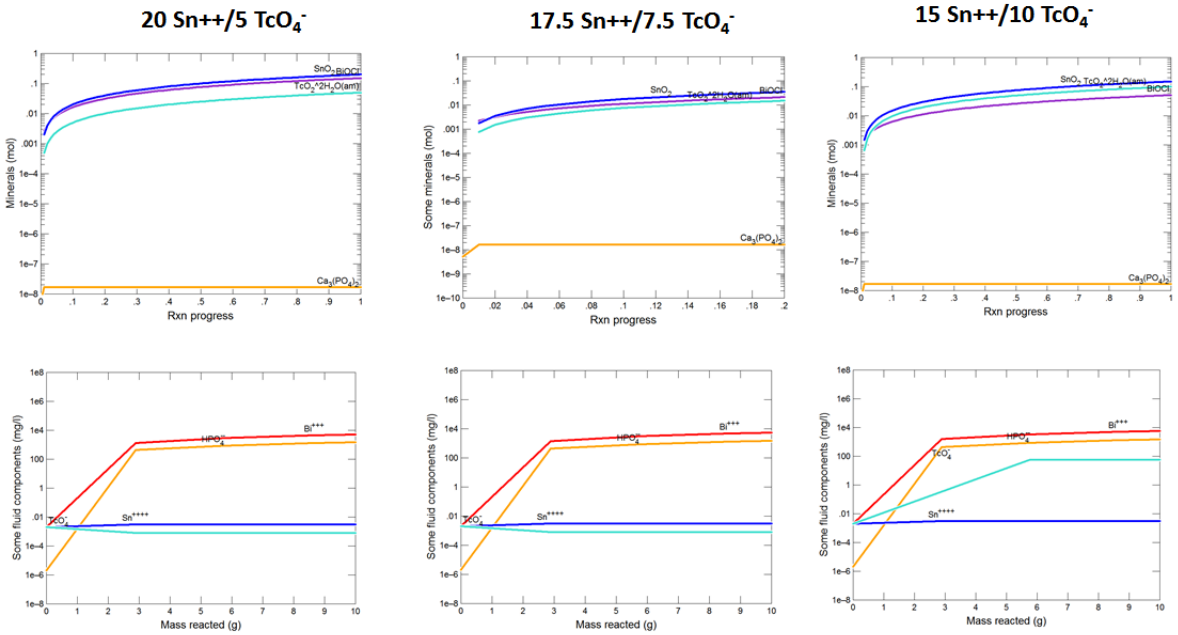

Figure 16. (a) Secondary phases predicted to form as a function of reaction progress (1 mol glass/L) (top); (b) Solution concentration for TcO_4^- (light blue), Sn^{4+} (dark blue), Bi^{3+} (red), and HPO_4^{2-} (orange) as a function of mass reacted at various composition of glass system (bottom).

Bi-Na-P + Sn(II) + $TcO_2 \cdot H_2O$

- Input glass composition: (mol%) 75 base material (Bi-Na-P), (25-x) SnO, x $TcO_2 \cdot 2H_2O$
- Reaction condition: 1 mol of glass reacts with 1000 ml DI water at near neutral pH

Results of the modeling are presented in terms of the secondary phases calculated to form as a function of reaction progress (1mol glass/L) (Figure 17a) and model results for selected elements as a function of mass reacted (Figure 17b).

Results indicate that at 5 mol% SnO, there is sufficient reducing agent to immobilize 20 mol% $TcO_2 \cdot 2H_2O$. As for other Tc(IV) simulations, $TcO_2 \cdot H_2O$ was oxidized first by O_2 to TcO_4^-, then reduced and immobilized.

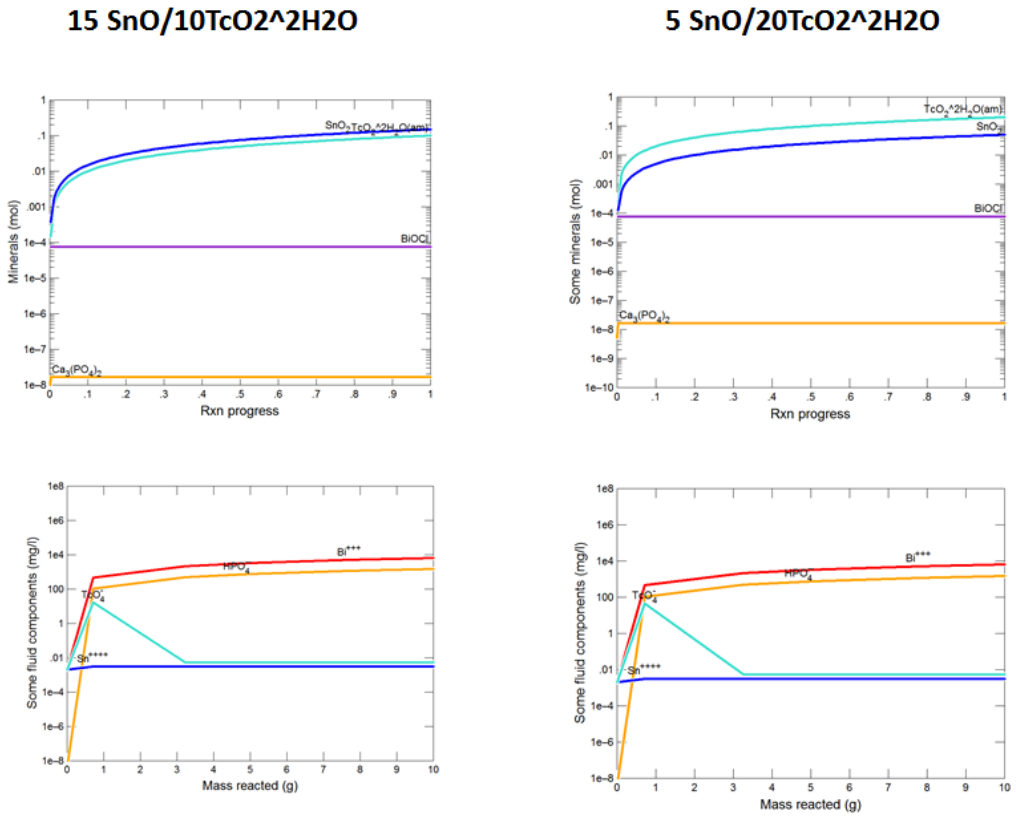

Figure 17. (a) Secondary phases predicted to form as a function of reaction progress (1 mol glass/L) (top); (b) Solution concentration for TcO_4^- (light blue), Sn^{4+} (dark blue), Bi^{3+} (red), and HPO_4^{2-} (orange) as a function of mass reacted at various composition of glass system (bottom) .

Bi-Ca-P + Sn(II) + $NaTcO_4$

- Input glass composition: (mol%) 75 base material (Bi-Ca-P), (25-x) Sn^{2+}, x TcO_4^-
- Reaction condition: 1 mol of glass reacts with 1000 ml DI water at near neutral pH

Results of the modeling are presented in terms of the secondary phases calculated to form as a function of reaction progress (1 mol glass/L) (Figure 18a) and model results for selected elements as a function of mass reacted (Figure 18b).

Results indicate that at 15 mol% Sn^{2+}, there is insufficient reducing agent to immobilize 10 mol% TcO_4^-. At 17.5 mol% Sn^{2+} and above, 7.5 mol% TcO_4^- can be immobilized. The corresponding mole ratios are expected to immobilize technetium at lower levels in the glass.

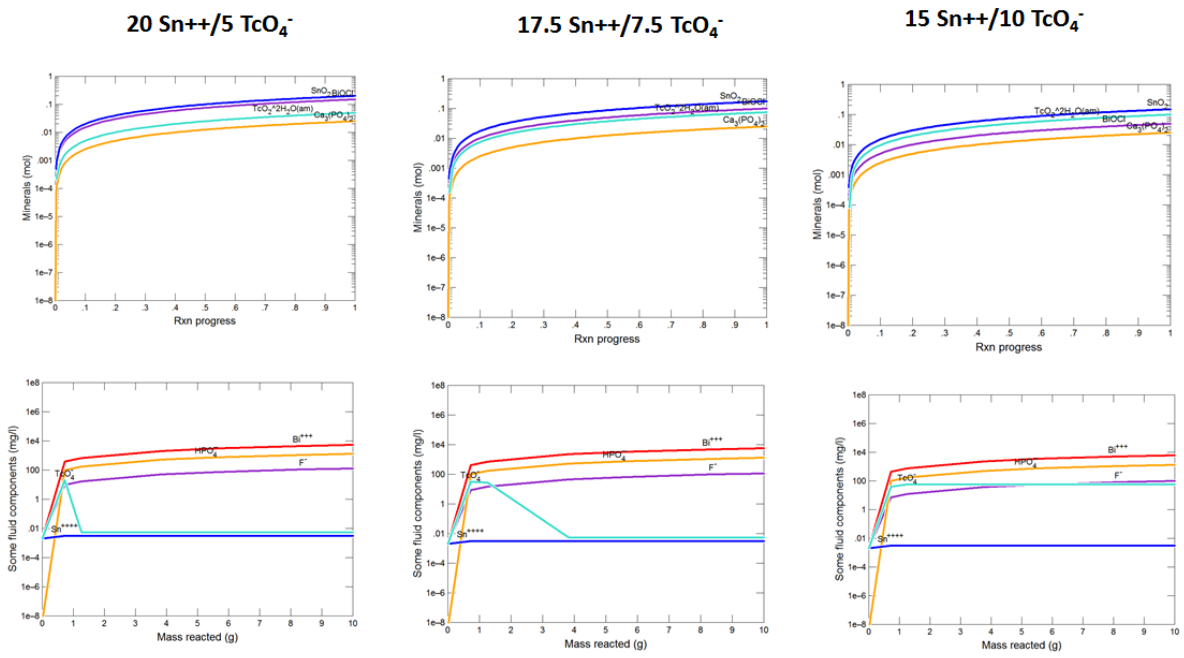

Figure 18. (a) Secondary phases predicted to form as a function of reaction progress (1mol glass/L) (top); (b) Solution concentration for TcO_4^- (light blue), Sn^{4+} (dark blue), Bi^{3+} (red), F^- (purple) and HPO_4^{2-} (orange) as a function of mass reacted at various composition of glass system (bottom).

Bi-Ca-P + Sn(II) + $TcO_2 \cdot H_2O$

- Input glass composition: (mol%) 75 base material (Bi-Ca-P), (25-x) SnO, x $TcO_2 \cdot 2H_2O$
- Reaction condition: 1 mol of glass reacts with 1000 ml DI water at near neutral pH

Results of the modeling are presented in terms of the secondary phases calculated to form as a function of reaction progress (1mol glass/L) (Figure 19a) and model results for selected elements as a function of mass reacted (Figure 19b).

Results indicate that at 5 mol% SnO, there is sufficient reducing agent to immobilize 15 mol% $TcO_2 \cdot 2H_2O$. As for other Tc(IV) simulations, $TcO_2 \cdot H_2O$ was oxidized first by O_2 to TcO_4^-, then reduced and immobilized.

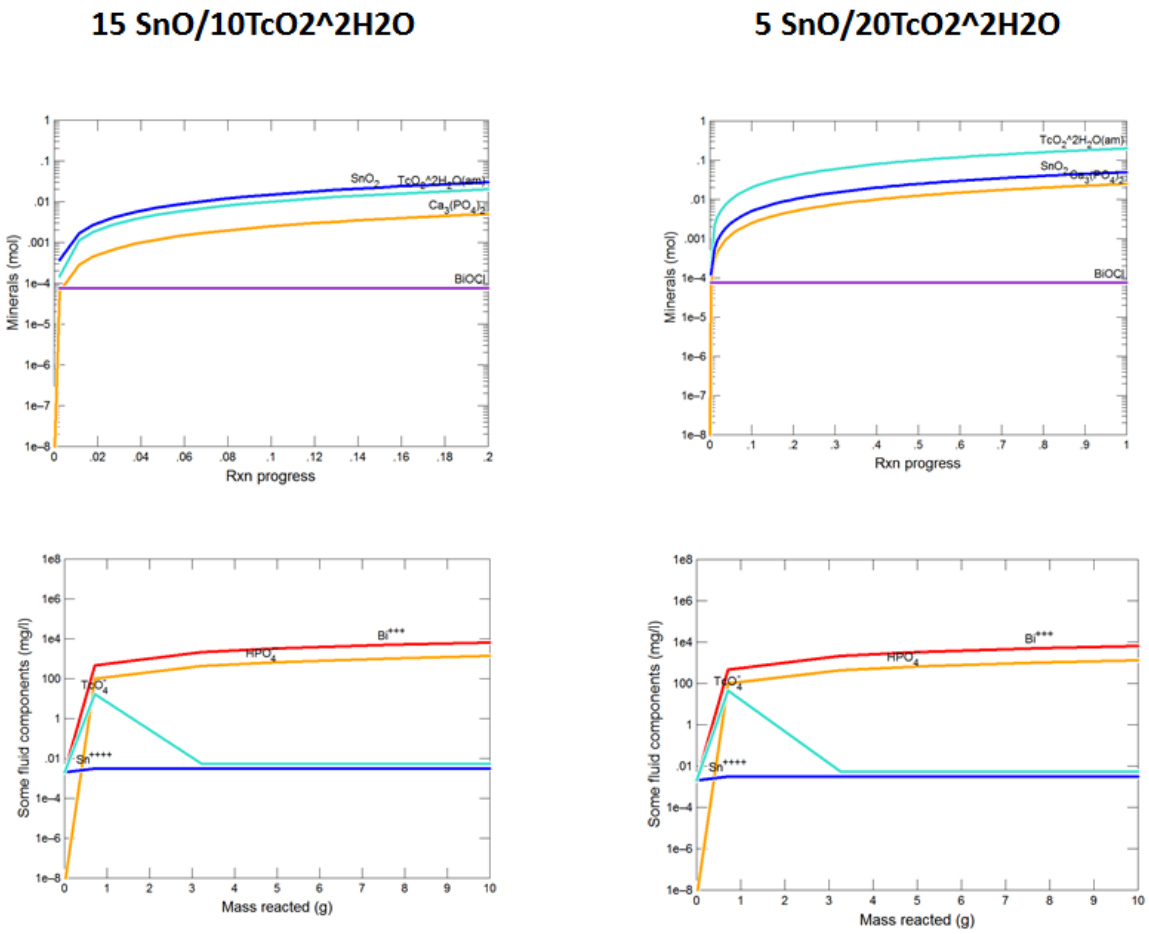

Figure 19. (a) Secondary phases predicted to form as a function of reaction progress (1 mol glass/L) (top); (b) Solution concentration for TcO_4^- (light blue), Sn^{4+} (dark blue), Bi^{3+} (red), and HPO_4^{2-} (orange) as a function of mass reacted at various composition of glass system (bottom) .

Pb-B + Sn(II) + $NaTcO_4$

- Input glass composition: (mol%) 75 50 PbO/50 B_2O_3, (25-x) SnO, x $NaTcO_4$
- Reaction condition: 1 mol of glass reacts with 1000 ml DI water at near neutral pH

Results of the modeling are presented in terms of the secondary phases calculated to form as a function of reaction progress (1mol glass/L) (Figure 20a) and the model results for solution concentrations (mg/L, as a function of mass reacted (Figure 20b).

Results indicate that at 15 mol% SnO, there is insufficient reducing agent to immobilize 10 mol% $NaTcO_4$. At 20 mol% SnO, 5-10 mol% $NaTcO_4$ can be immobilized.

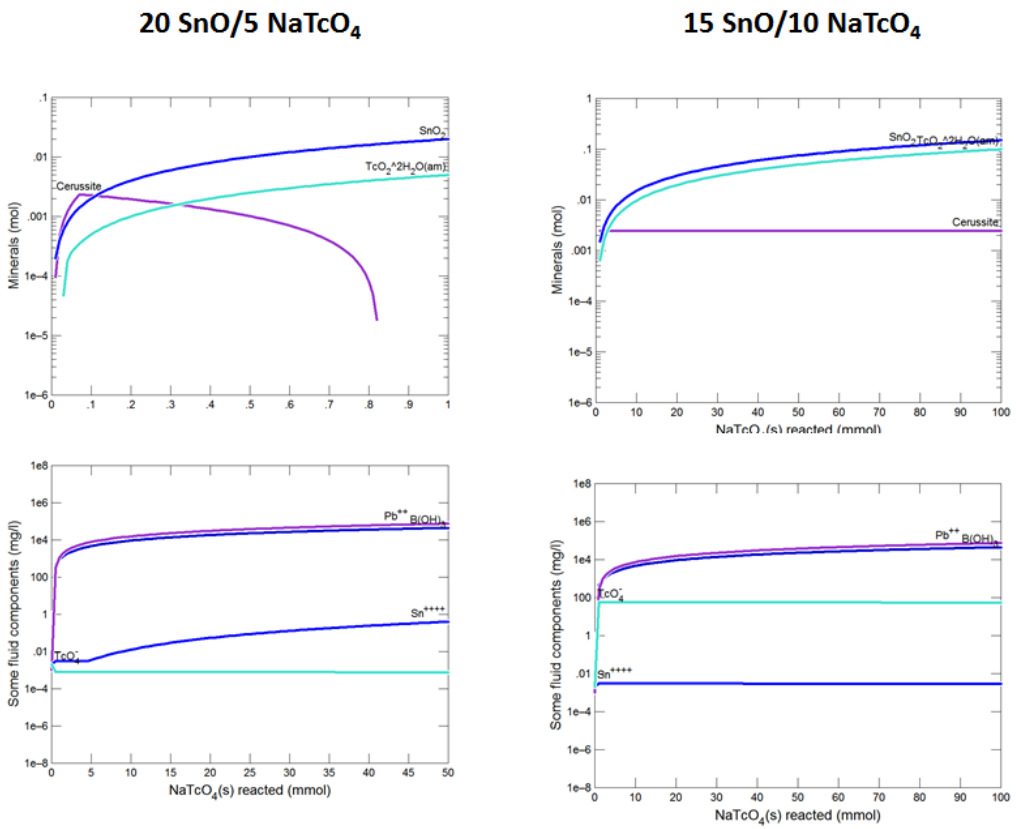

Figure 20. (a) Secondary phases predicted to form as a function of reaction progress (1mol glass/L) (top); (b) Solution concentration for TcO_4^- (light blue), Sn^{4+} (dark blue), Pb^{2+} (purple), and $B(OH)_3$ (blue, purple) as a function of mass reacted at various composition of glass system (bottom).

Pb-B + Sn(II) + $TcO_2 \cdot H_2O$

- Input glass composition: (mol%) 75 50PbO/50 B2O3, (25-X) SnO, X $TcO_2 \cdot 2H_2O$
- Reaction condition: 1 mol of glass reacts with 1000 ml DI water at near neutral pH

Results of the modeling are presented in terms of the secondary phases calculated to form as a function of reaction progress (1 mol glass/L) (Figure 21a) and the model results for solution concentrations (mg/L, as a function of mass reacted (Figure 21b).

Results indicate that at 1 mol% SnO and above, there is sufficient reducing agent to immobilize 24 mol% $TcO_2 \cdot 2H_2O$. The result also indicate at 5 mol% SnO and below, Tc(IV) was oxidized first by O_2 to TcO_4^- , then reduced and immobilized.

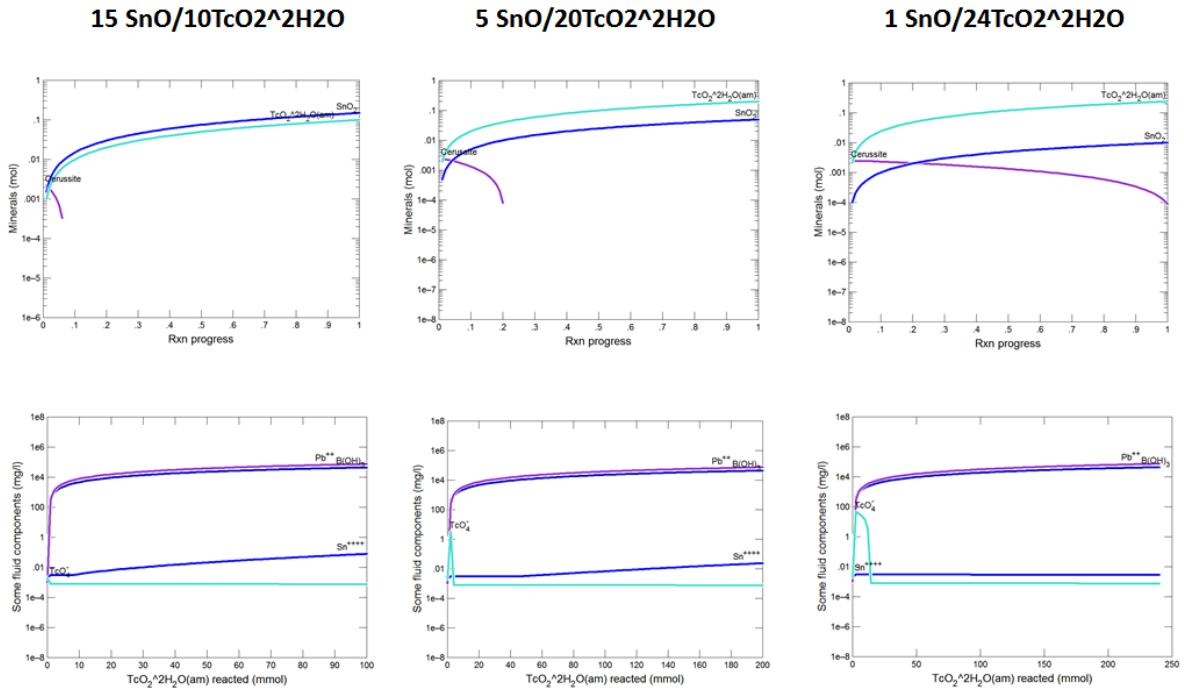

Figure 21. (a) Secondary phases predicted to form as a function of reaction progress (1 mol glass/L) (top); (b) Solution concentration for TcO_4^- (light blue), Sn^{4+} (dark blue), Pb^{2+} (purple), and $B(OH)_3$ (blue, purple) as a function of mass reacted at various composition of glass system(bottom).

Conclusions of Geochemical Modeling Study

The geochemical modeling examined the fate of the technetium waste forms in equilibrium with water and unlimited oxygen. With oxygen present in every simulation, the technetium is ultimately released as pertechnetate from every simple combination of technetium and glass, except that of the reducing Sn-Pb-P glass. If low-melting compositions of this glass have sufficient phase stability and chemical durability, it may be possible to secure a sodium pertechnetate-containing eluate in this reducing glass.

For all other glasses, the presence of SnO or SnF_2 at the appropriate stoichiometry provides the thermodynamic stability needed to maintain technetium as its insoluble oxide. Not surprisingly, a much smaller quantity of Sn^{2+} reducing agent is required to immobilize the Tc(IV) oxide than the Tc(VII) pertechnetate ion. While this modeling approach cannot address this directly, it is possible that even a sub-stoichiometric amount of divalent tin can greatly reduce the rate of release of technetium from a waste form. This finding suggests that the precipitated TcO_2/Sn/Cr solid can be effectively immobilized in a variety of glass or glass-composite matrices, because a significant mass excess of Sn is present in the precipitate [Taylor-Pashow 2015]. Measurement of the Sn oxidation state and the Tc leaching rate from this precipitate (without immobilization in glass) would help confirm this hypothesis.

Summary of Recommendations

In Table 4, we summarize and assign a relative technical risk for each the processing routes available to address each of the three possible recovered streams using a low-temperature glass. The processing route assessed to have the lowest technical risk for $NaTcO_4$ in an aqueous anion exchange eluent is vitrification in a low-melting glass, such as the Pb-B or Sn-Pb-P formulations. For a $TcO_2 \cdot 2H_2O$ slurry arising from precipitation technetium (and chromium) with stannous chloride, we recommend encapsulation in a glass-composite material using a low-firing glass such as the bismuth-based electronics glasses as the lowest-risk approach. Because it is difficult to anticipate the effect of the non-elutable anion exchange resin on glass or CGM waste forms, none of the processing options for this feed are rated better than moderate technical risk at this time.

The recommended overall priority for evaluation and development of alternative glass waste forms is:

1. **Encapsulation of precipitated TcO_2/Sn/Cr in a glass composite material based on the Ferro EG 2922 Bi-Si-Zn glass**. This glass is well-demonstrated at the bench scale to have the processing temperatures and high durability required for waste encapsulation, and extending this work to technetium immobilization is straightforward. Addition of divalent tin oxide to the GCM formulation can provide additional assurance that pertechnetate will not leach out of the waste form, and durability can be further extended by surrounding the GCM with additional glass in a core/shell structure. Technical issues to be addressed at the bench scale include chromium and technetium mobility; influences of waste and divalent tin loadings on thermomechanical properties of the GCM; and development of a pretreatment approach to ensure that minimal off-gassing occurs during the pressing and sintering of the waste. The best current alternatives to this glass are Bi-Ca-P or Bi-Na-P, which contain no RCRA LDR-regulated species. Risk can be further mitigated by a small concurrent effort to screen other commercial sealing glasses for their durability. Development and scale-up issues include mechanical durability and homogeneity of GCM waste forms, which have not been demonstrated above laboratory scale.

2. **Vitrification of $NaTcO_4$ in aqueous anion exchange eluent solution using a high lead content borate glass, or other low melting glass.** Vitrification is the least complex route to immobilization of this technetium feed, and at this time, unmodified lead borate glass has the best known combination of processing temperature and chemical durability. Compatibility of the sodium nitrate-based feed with this melt glass composition should be screened at different waste loading levels to verify that a stable vitreous product is obtained, and if successful, sodium perrhenate or pertechnetate should next be added to the glass formulation to begin durability testing. If the processing temperature, phase stability, or durability of this glass is insufficient for the proposed application, another good candidate for continued development is the Sn-Pb-P glass. This glass currently lags in our recommendation mainly because of its high sensitivity to compositional changes, but its lower Pb content and incorporation of Tc-stabilizing stannous ion are potential benefits in this application. Risk can be further mitigated by a small effort to determine the applicability (e.g., melting/viscosity and durability characteristics) of the B-Al-Na glasses in the composition range >60 mol% B_2O_3, <20% Na_2O and <20% Al_2O_3.

Development and scale-up issues to be addressed for this process category include: atmosphere control for Sn(II)-containing glasses; effects of eluate salts (chloride, sulfate) on glass durability; and industrial health and safety controls for lead-containing glasses.

For all chemical durability testing of these glasses, it is important to measure leaching from both powders and monoliths using the PCT-B and MCC-1 standard tests. Any glasses that contain RCRA elements must also pass the LDR TCLP standard before being developed further. Additional experimentation is required before a low-temperature glass waste form can be recommended for technetium absorbed on the non-elutable resin.

Table 4. Summary table of processing routes for the three technetium feed streams. For each potential combination, an assessment is made of suitability and technical risk. Priority glass types are identified, and key areas of technical advantage and risk are briefly identified.

	Recovered Tc Stream		
Immobilization Process	**A-530E resin** Organic resin in a water slurry	**SL-639 IX eluate** Water solution with dissolved salts	**Precipitated Tc/Sn/Cr** Water slurry with precipitated solids
Low temperature vitrification (700 °C) Recovered Tc stream is dissolved in molten glass	**Medium technical risk** Sn-Pb-B-P-X Pb-B - Effect of carbon on melting temperature and durability? - Composition greatly affects durability of Sn-Pb-B-P-X	**Lower technical risk** Sn-Pb-B-P-X Pb-B - Lead borate glass has good durability for Cs, Sr incorporation - Tin(II) glass may help immobilize Tc, but composition greatly affects durability - Effects of sulfate, chloride unknown	**Medium technical risk** Pb-B Sn-Pb-B-P-X - TcO_2 may be less likely to volatilize than TcO_4^- - Composition greatly affects durability of Sn-Pb-B-P-X - Potential for Cr release
Low temperature encapsulation (500-600 °C) Recovered Tc stream is sealed within a glass composite material by low-temperature sintering	**Higher technical risk** Bi-Na-P (M=Na) B-Al-Na - Effect of carbon on sealing temperature and durability?	**Not recommended** Aqueous feed is not suitable for encapsulation, unless dried	**Lower technical risk** Bi-Si-Zn Bi-B-Zn Bi-M-P (M=Ca, Na) - Literature precedent for ^{129}I encapsulation - Some durability data - Variety of commercial materials - Potential for Cr release
Very low temperature immobilization (<200 °C) Recovered Tc stream is chemically immobilized in glass via sol-gel	**Higher technical risk** Sol-gel - Suspend resin - Durability unknown	**Medium technical risk** Sol-gel - Lowest temperatures - Durability unknown	**Not recommended** Dense solid oxide feed is least suited to sol-gel encapsulation.

Literature Cited

[3M 2017a] 3M Advanced Materials Division, “3M specialty glass: lead-free,” http://multimedia.3m.com/mws/media/951209O/3m-specialty-glass-lead-free-data-sheet.pdf (retrieved 5/12/17).

[3M 2017b] 3M Advanced Materials Division, “3M specialty glass for low temperatures,” http://multimedia.3m.com/mws/media/951219O/3m-specialty-glass-for-low-temperatures-data-sheet.pdf (retrieved 5/12/17).

[40 CFR 268] Title 40 - Protection of Environment, Part 268 – Land Disposal Restrictions. https://www.gpo.gov/fdsys/pkg/CFR-2012-title40-vol28/xml/CFR-2012-title40-vol28-part268.xml

[ASTM C338] ASTM C338 - 93(2013), “Standard test method for softening point of glass,” https://www.astm.org/Standards/C338.htm

[ASTM C965] ASTM C965 - 96(2012),”Standard practice for measuring viscosity of glass above the softening point,” https://www.astm.org/Standards/C965.htm

[ASTM C1220] ASTM C1220 – 10 “Standard test method for static leaching of monolithic waste forms for disposal of radioactive waste,” https://www.astm.org/Standards/C1220.htm

[ASTM C1285] ASTM C1285 – 14 “Standard test methods for determining chemical durability of nuclear, hazardous, and mixed waste glasses and multiphase glass ceramics: the product consistency test (PCT),” https://www.astm.org/Standards/C1285.htm

[Bajaj 2013] Bajaj, A.; Khanna, A.; Krishnan, K.; Aggarwal, S. K. *Phase Transitions, 86* (2013) 541-500.

[Bengisu 2016] Bengisu, M. “Borate glasses for scientific and industrial applications: a review,” *J. Mater. Sci.*, *51* (2016) 2199–2242.

[Brown 2017] Brown, H., 3M Corporation, personal communication: “Low temperature glasses,” 2017.

[Cao 1995] Cao, H.; Adams, J. W.; Kalb, P. D. “Low Temperature Glasses for Hanford Tank Wastes,” Brookhaven National Laboratory Report BNL-52595, June 1995.

[Childs 2015] Childs B.; Poineau F.; Czerwinski K.; Sattelberger A. “The nature of the volatile technetium species formed during vitrification of borosilicate glass,” *J. Radioanal. Nucl. Chem. 306* (2015) 417–421.

[Crum 2014] Crum, J.; Maio, V.; McCloy, J.; Scott, C.; Riley, B.; Benefiel, B.; Vienna, J.; Archibald, K.; Rodriguez, C.; Rutledge, V.; Zhu, Z.; Ryan, J.; Olszta, M. “Cold crucible induction melter studies for making glass ceramic waste forms: A feasibility assessment,” *J. Nucl. Mater. 444* (2014) 481-492.

[Darab 1996] Darab, J. G.; Smith, P. A. “Chemistry of technetium and rhenium species during low-level radioactive waste vitrification,” *Chem. Mater. 8* (1996) 1004-1021.

[Deptula 2011] Deptula, A.; Milkowska, M.; Lada, W.; Olczak, T.; Wawszczak, D.; Smolinski, T.; Zaza, F.; Brykala, M.; Chmielewski, A. G.; Goretta, K. C. “Sol-gel processing of silica nuclear waste glasses,” *New J. Glass. Ceram.*, *1* (2011) 105-111.

[Ding 2014] Ding, M.; Lu, C.; Cui, Q.; Ni, Y.; Xu, Z. “Fabrication and characterization of B_2O_3-Al_2O_3-Na_2O glass system for transparent dielectric layer,” *Ceramics Intl.*, *40* (2014) 233-239.

[DOE 2001] U.S. Department of Energy (DOE). 2001. “Design, Construction, and Commissioning of the Hanford Tank Waste Treatment and Immobilization Plant,” DOE Office of River Protection, Richland, WA; Contract with Bechtel National, Inc., San Francisco, CA, Contract No.: DE-AC27-01RV14136 (As quoted in http://www.pnl.gov/main/publications/external/technical_reports/PNNL-14251.pdf).

[Donald 2006] Donald, I. W.; Metcalfe, B. L.; Fong, S. K.; Gerrard, L. A. “The influence of Fe_2O_3 and B_2O_3 additions on the thermal properties, crystallization kinetics and durability of a sodium aluminum phosphate glass,” *J. Non-Cryst. Solids*, *352* (2006) 2993–3001.

[Doweider 2001] Doweidar, H.; Moustafa, Y. M.; Abd El-Maksoud, S.; Silim, H. “Properties of Na_2O–Al_2O_3–B_2O_3 glasses,” *Mater. Sci. Eng.*, *A301* (2001) 207-212.

[Dumesnil 1993] Dumesnil, M. E.; Finkelstein, L. “Low temperature sealing glass compositions,” US Patent 1993/5188990 A, published Feb 23, 1993.

[EPA 1311] Test Method 1311: Toxicity Characteristic Leaching Procedure. Hazardous Waste Test Methods / SW-846. https://www.epa.gov/sites/production/files/2015-12/documents/1311.pdf

[Erdogan 2014] Erdogan, C.; Bengisu, M.; Erenturk, S. A. “Chemical durability and structural analysis of PbO–B2O3 glasses and testing for simulated radioactive wastes,” *J. Nucl. Mater.*, *445* (2014) 154-164.

[Ferro 2017] Ferro Electronic Materials, “Low-temperature Pb-free glasses,” http://www.ferro.com/non-cms/ems/EPM/content/docs/Low%20Temp%20Pb-Free%20Glasses.pdf (retrieved 5/12/2017).

[Garino 2011] Garino, T. J.; Nenoff, T. M.; Krumhansl, J. L.; Rademacher, D. X. “Low-Temperature Sintering Bi–Si–Zn-Oxide Glasses for Use in Either Glass Composite Materials or Core/Shell ^{129}I Waste Forms,” *J. Am. Ceram. Soc., 94* (2011) 2412–2419.

[Gibson 1993] Gibson, J. K. “Mass spectrometric identification of gaseous potassium and cesium pertechnetates and bimetallic technetium-rhenium oxide dimers,” *Radiochim. Acta, 62* (1993) 127.

[Gombert 2003] Gombert, D.; Richardson, J. R. “Cold-crucible induction melter design and development”, *Nucl. Technol., 141* (2003) 301-308.

[He 2016a] He, F.; He, Z.; Xie, J.; Mei, S.; Jin, M. “Melting, sintering and wetting properties of ZnO-Bi_2O_3-B_2O_3 sealing glass, *J. Cent. South Univ.*, *23* (2016) 1541-1547.

[He 2016b] He, P.; Guo, W.; Lin, T.-S.; Lin, P.-P. “Progress in research on green lead-free low-melting sealing glasses,” *J. Mater. Eng.*, *44* (2016) 123-130.

[Hormadaly 2006] Hormalady, J. “Lead-free phosphate glasses,” US Patent 2006/0128549 A1, published Jun 15, 2006.

[Hu 1994] Hu, L.; Jiang, Z. “Formation and Properties of Tin(II) Chlorophosphate Glasses,” *Phys. Chem. Glasses*, *35* (1994) 38-41.

[Jacq 2006] Jacq, C.; Maeder, T.; Martinerie, S.; Corradini, G.; Carreno-Morelli, E.; Ryser, P. "High performance thick-film pressure sensors on steel," 4th European Microelectronics and Packaging Symposium, 2006.

[Jacq 2009] Jacq, C.; Maeder, T.; Ryser, P. “Development of low-firing lead-free thick-film materials on steel alloys for piezoresistive sensor applications,” Microelectronics and Packaging Conference, 2009. http://ieeexplore.ieee.org/document/5272900/

[Kajihara 2013] Kajihara, K. “Recent advances in sol–gel synthesis of monolithic silica and silica-based glasses,” *J. Asian Ceram. Soc.*, *1* (2013) 121-133.

[Kikuchi 1999] Kikuchi, M.; Yoshida, T.; Matsuda, M.; Kanai, H. “Developing technologies for nuclear fuel cycles—radioactive waste treatment and spent fuel storage,” *Hitachi Review*, *48* (1999) 277-284.

[Liu 2012] Liu, Y.; Deng, D.; Wang, H.; Zhao, S.; Xu, S. “Effect of Oxides Additive on Properties and Structure of Low-Melting Sealing Bi_2O_3-B_2O_3-ZnO Glasses,” *J. Chinese Ceram. Soc.*, *40* (2012) 1409-1414.

[Marra 2014] Marra, J. C.; Ojovan, M. I. “Vitrification of radioactive wastes – a current solution and enabler for future nuclear technologies”; Report STI-2014-00075, United States Department of Energy, Savannah River Site, 2014.

[Maeder 2013] Maeder, T. “Review of Bi_2O_3 based glasses for electronics and related applications,” *Int. Mater. Rev.*, *58* (2013) 3-40.

[Minteq 2006] USEPA’s Minteq2: A geochemical Assessment Model for Environmental Systems, v4.0.

[Mowry 2015] Mowry, C. D.; Brady, P. V.; Garino, T. J.; Nenoff, T. M. “Development and Durability Testing of a Low-Temperature Sintering Bi–Si–Zn Oxide Glass Composite Material (GCM) ^{129}I Waste Form,” *J. Am. Ceram. Soc*. *98* (2015) 3094–3104.

[Naito 2011] Natio, T.; Aoyagi, T.; Sawai, Y.; Tachizono, S.; Yoshimura, K.; Hashiba, Y.; Yoshimoto, M. Japan. J. Applied Phys., 50 (2011) 088002.

[Norman 1998] Norman, N. C. *Chemistry of Arsenic, Antimony and Bismuth*, Springer, 168-170, 1998.

[NRC 2011] NRC Committee on Waste Forms Technology and Performance, “Waste Forms Technology and Performance: Final Report,” Division on Earth and Life Studies, Nuclear and Radiation Studies Board, National Academies Press, Sep 5, 2011.

[Ojovan 2007] Ojovan, M.I.; Batyukhnova, O.G.; “Glasses for Nuclear Waste Immobilization”; WM’07 Conference, February 25-March 1, 2007, Tucson, AZ.

[Pan 1995] Pan, Z.; Morgan, S. H.; Long, B. H. *J. Non-Cryst. Solids, 185* (1995) 127-134.

[Pauling 1988] Pauling, L.C., *General Chemistry*, Dover Publications, 1988.

[Pegg 2015] Pegg, I. L, *J. Radioanal. Nucl. Chem.*, *305* (2015) 287-292.

[Perera 2004] Perera, D. S.; Vance, E. R.; Trautman, R. L.; Begg, B. D. "Current Research on I-129 Immobilization," WM'04 Conference, WM-4089 (2004).

[Pierce 2011] Pierce, E. M.; Bacon, D. H.; Kerisit, S. N.: Windisch, Jr. C. F.; Cantrell, K. J.; Valenta, M. M.; Burton, S. D. “Integrated Disposal Facility FY2011 Glass Testing Summary Report,” Report PNNL-20781, Pacific Northwest National Laboratory, 2011.

[Raj 2006] Raj , K.; Prasad, K. K.; Bansal, N. K. “Radioactive waste management practices in India,” *Nucl. Eng. Design*, *236* (2006) 914–930.

[Rard 1999] Rard, J.A.; Rand, M.H.; Anderegg, G.; Wanner, H. “Chemical Thermodynamics of Technetium”, Sandino, A.M.C. and östhols, E. (editors), OECD Nuclear Energy Agency, Elsevier, 1999.

[Rard 2005] Rard, J.A. “Current status of the thermodynamic data for technetium and its compounds and aqueous species”, *J. Nucl. Radiochem. Sci*., *6*, (2005) 197-204.

[Ren 2008] Ren, Y.; Feng, S.; Hu, S.; Yang, Q. "The development test of lead-free aluminum low-temperature sealing glass," The 7th National Conference on Functional Materials and Applications, (2010) 2085-2088.

[Riley 2016] Riley, B. J.; Vienna, J. D.; Strachan, D. M.; McCloy, J. S. “Materials and processes for the effective capture and immobilization of radioiodine: A review,” *J. Nucl. Mater.*, *470* (2016) 307-326.

[Ringwood 1981] Ringwood, A.E.; Oversby, V.M.; Kesson, S.E.; Sinclair, W.; Ware, N.; Hibberson, W.; Major, A. “Immobilization of high-level nuclear reactor wastes in Synroc: a current appraisal”, *Nucl. Chem. Waste Management, 2* (1981) 287-305.

[Roach 2008] Roach, J. A.; Lopukh, D. B.; Martynov, A. P.; Polevodov, B. S.; Chepluk, S. I. “Advanced modeling of cold crucible induction melting for process control and optimization,” Waste Management 2008 Conference Preprint, Report INL/CON-08-13730, February 2008.

[Robbins 2013] Robbins, R. A., May, T. H.. 2013. “Submerged Bed Scrubber Condensate Technetium Removal and Disposal Preconceptual Engineering Study.” RPP-RPT-55213, Washington River Protection Solutions, Richland, WA, 2013.

[Rutledge 2013] Rutledge, V. J.; Maio, V. “The production of advanced glass ceramic HLW forms using cold crucible induction melter,” Preprint INL/CON-13-28244, GLOBAL 2013 conference, October 2013.

[Sava 2012] Sava, D. F.; Garino, T. J.; Nenoff, T. M. “Iodine confinement into metal-organic frameworks (MOFs): low-temperature sintering glasses to form novel glass composite material (GCM) alternative waste forms,” *Ind. Eng. Chem. Research*, *51* (2012) 614–620.

[Serne 2014] Serne, R. J.; Rapko, B. M. “Technetium inventory, distribution, and speciation in Hanford tanks,” Report PNNL-23319, May 2014.

[Shih 2001] Shih, P. Y.; Chin, T. S. “Preparation of lead-free phosphate glasses with low T_g and excellent chemical durability,” *J. Mater. Sci. Lett.*, *20* (2001) 1811-1813.

[Taylor-Pashow 2015] Taylor-Pashow, K. M. L.; McCabe, D. J. “Laboratory optimization tests of technetium decontamination of Hanford waste treatment plant low activity waste melter off-gas

condensate simulant," Report SRNL-STI-2015-00645, Savannah River National Laboratory, November 2015.

[Takebe 2006] Takebe, H.; Baba, Y.; Kuwabara, M. "Dissolution behaviour of ZnO-P2O5 glasses in water," *J. Non-Crystal. Solids*, *352* (2006) 3088-3094.

[Tick 1984] Tick, P. A. "Water durable glasses with ultra low melting temperatures," *Phys. Chem. Glasses*, *25* (1984) 149-154.

[Totokawa 2009] Totokawa, M.; Yamashita, S.; Morikawa, K.; Mitsuoka, Y.; Tani, T.; Makino, H. "Microanalyses on the RuO_2 Particle-Glass Matrix Interface in Thick-Film Resistors with Piezoresistive Effects," *Int. J. Appl. Ceram. Technol.*, *6* (2009)195–204.

[Uchida 2001] Uchida, S.; Tagami, K. "Low-level technetium-99 determination in soil samples by ICP-MS." Radiochemical Measurements Conference, Honolulu HI, Nov 3-8, 2001. http://www.lanl.gov/BAER-Conference/BAERCon-47p-Uchida1.pdf

[Valenta 2010] Valenta, M. M.; Parker, K. E.; Pierce, E. M. "Tc-99 ion exchange resin testing," Report PNNL-19681, August 2010.

[Westsik 2014] Westsik, J. H., Jr; Cantrell, K. J.; Serne, R. J.; Qafoku, N. P. "Technetium Immobilization Forms: Literature Survey," Report PNNL-23329, May 2014.

[Yamanaka 2002] Yamanaka T. "Lead-free tin silicate phosphate glass and sealing material containing the same," US Patent 2002/0019303 A1, published Feb 14, 2002.

[Yang 2013] Yang, J. H.; Shin, J. M.; Park, J. J.; Park. H. S. "I-129 waste form using Bi-Zn-P-oxide glass," *Energy Procedia*, *39* (2013) 151-158.

[Yang 2014] Yang, J. H.; Shin, J. M.; Park, J. J.; Park, G. I. "Waste form of silver iodide (AgI) with low-temperature sintering glasses," *Sep. Sci. Technol., 49* (2014) 298–304.

[Yang 2016] Yang, J. H.; Park, H. S.; Ahn, D.-H.; Yim, M.-S. "Glass composite waste forms for iodine confined in bismuth-embedded SBA-15," *J. Nucl. Mater.*, *480* (2016) 150–158

[Zelinski 1998] Zelinski, B. J. J.; Young, J.; Davidson, D.; Aruchamy, A.; Uhlmann, D. R.; Smith, G. L.; Smith, H. D. "Sol-gel technology and the nuclear industry," Waste Management 1998 Conference Preprint, http://www.wmsym.org/archives/1998/html/sess09/09-31/09-31.htm.

Acknowledgements

Dr. George S. Goff and Dr. Paul R. Dixon are thanked for helpful technical and programmatic discussions. Photographs of LANL sol-gel materials were provided by Dr. Gautam Gupta and his research team.

Appendix A. Typical Properties of Low-Temperature Glass Families

Listed in order of increasing melting/sintering temperature, based on available measurements. Incomplete data makes relative positions unreliable.

Glass Family	Melting Point (°C)	Sintering Temp (°C)	Softening Point (°C)	Transition Temp (T_g °C)	Vitreous/ Crystallizing	Detail Composition	Comments	Citation
Bi-B-Zn-Al		<550	<490	<470		20.3, 45.3, 19.4, 2.2	Sintering temp. <550C	Liu 2012
Bi-P-Zn		600				varies	Some dissolution data.	Yang 2013
Pb-B-Si			350-450			varies		He 2016b
P-Al-B-R			375-410	295-315		41-56, 1-4, 1-7, 40-50 RE		Ren 2008
Zn-B-P			<400	280-500		varies		He 2016b
V-P-Sb			<400	<330		varies		He 2016b
Sn-Zn-P			<400	<350		varies		He 2016b
Pb-B-Zn			400-580	280-520		varies		He 2016b
K-B-Bi			430-470	360-410		varies		He 2016b
Bi-B-Zn			<450	<400		varies		He 2016b
Pb-B-Si-Al			463-545	375-440	Vitreous	65-73, 18-28, 4-5, 3-4	Some dissolution data.	Erdogan 2014
Bi-B-Ba			490-512	458-481		varies		He 2016b
V-P-Ca			<500	170-300		varies		He 2016b
Sn-Si-P			<500	250-350		varies		He 2016b
V-Te-Sn			<500	250-400		varies		He 2016b
V-B-Zn			<500	280-330		varies		He 2016b
Sn-B-P			<500	280-380		varies		He 2016b
Zn-Nb-P			<500	<450		25-37; 0.1-15; 40-65		Hormadaly 2006
Bi-Ba-Si			<500	<475		varies		He 2016b
B-Ca-Al				300-450		varies		He 2016b
V-B-Al				400-500		varies		He 2016b
Na-Zn-B-Si				450-510		varies		He 2016b
R-Al-Si-Bi				450-550		varies		He 2016b
Zn-P				<500		50-70, 30-50	Some dissolution data.	Takebe 2006
Na-Zn-B-Si				600-700		varies		He 2016b

Appendix B. Low-Temperature Glass Properties

Listed in order of increasing melting/sintering temperature, based on available measurements. Incomplete data makes relative ranking unreliable. Glasses identified as high priorities in this report are identified in bold type.

Glass Composition	Melting Point (°C)	Sintering Temp (°C)	Softening Temp (T_f °C)	Transition Temp (T_g °C)	Vitreous/ Crystallizing	Detail Composition	Comments	Citation
AgI-Ag2O-P2O5	400							Kikuchi 1999
Pb–Sn–P–O–F	**<450**			**95**		**6.4, 59, 34 metals**	**Some dissolution data**	**Tick 1984**
Pb–Sn–P–O–F	**<450**			**125**		**6.2, 57, 37 metals**	**Some dissolution data**	**Tick 1984**
Pb-B	**463**			**389**		**75, 25**	**0.30 g/m2/day**	**Erdogan 2014**
Pb-B	**465**			**393**		**80, 20**	**0.20 g/m2/day**	**Erdogan 2014**
Pb-B	**468**			**383**		**70, 30**	**0.28 g/m2/day**	**Erdogan 2014**
Sn-P-O-Cl	<500			181		50, 50	Hygroscopic	Hu 1994
Sn-P-O-Cl	<500			214		60, 40 (Cl/O varies)	Some dissolution data	Hu 1994
Pb-Sn-P-O-Cl	<500			222		5, 40, 55	Some dissolution data	Hu 1994
Sn-P-O-Cl	<500			222		65, 35	Some dissolution data	Hu 1994
Pb-B	545			410		40, 60	15 g/m2/day	Erdogan 2014
Bi-B-Zn-Si	600			430		not specified		Totokawa 2009
Na-Al-P-B	690			441		36.7, 17.5, 35.8, 10.0	5.12 wt% loss, 28d at 70°C	Donald 2006
Pb-B	>700			375		60, 40	.75 g/m2/day. Si/Al inclusion.	Erdogan 2014
Pb-B	>700			405		50, 50	21 g/m2/day	Erdogan 2014
Pb-B	>700			440		30, 70	26 g/m2/day	Erdogan 2014
Na-Al-P-B	734			433		38.7, 18.5, 37.8, 5.0	1.75 wt% loss, 28d at 70°C	Donald 2006
Na-Al-P-B	740			428		40.4, 19.2, 39.4, 1.0	1.09 wt% loss, 28d at 70°C	Donald 2006
Na-Al-P	741			405		40.8, 19.4, 39.8	1.50 wt% loss, 28d at 70°C	Donald 2006
Na-Al-P-B	742			427		40.0, 19.0, 39.0, 2.0	1.74 wt% loss, 28d at 70°C	Donald 2006
Na-Al-P-B	742			428		40.2, 19.1, 39, 1.5	1.13 wt% loss, 28d at 70°C	Donald 2006
Na-Al-P-B	747			427		40.6, 19.3, 39.6, 0.5	1.34 wt% loss, 28d at 70°C	Donald 2006
Sn-Si-P-Zn-Cs	750			259		47.9, 6.9, 30.0, 10.0, 5.2		Yamanaka 2002
Na-Al-P-Fe	777			437		37.9, 18.1, 40.5, 3.5	0.11 wt% loss, 28d at 70°C	Donald 2006
Na-Al-P-Fe	782			442		36.4, 17.4, 40.9, 5.3	0.07 wt% loss, 28d at 70°C	Donald 2006
Pb-Fe-P	800		500			20, 11, 65		Perera 2004
Sn-Si-P-Zn-Mn	800			250		44.9, 7.0, 34.2, 10.9, 3.0		Yamanaka 2002
Sn-Si-P-Zn-Sn	800			250		37.9, 6.0, 35.2, 10.9, 10.0		Yamanaka 2002
Sn-Si-P-Zn-B-Li	800			255		41.9, 6.9, 30.2, 10.0, 1.0, 10.0		Yamanaka 2002
Sn-Si-P-Zn	800			264		47.9, 8.0, 35.2, 8.9		Yamanaka 2002
Sn-Si-P-Zn-Cu	800			267		44.9, 7.0, 34.2, 10.9, 3.0		Yamanaka 2002
Sn-Si-P-Zn-Nb	800			271		46.9, 6.0, 35.2, 10.9, 1.0		Yamanaka 2002
Sn-Si-P-Zn-B	800			275		42.9, 6.0, 36.2, 10.9, 4.0		Yamanaka 2002
Sn-Si-P-Zn-B	800			278		47.9, 6.0, 33.2, 10.9, 2.0		Yamanaka 2002
Sn-Si-P-Zn-Mg	800			286		43.9, 7.0, 33.2, 7.9, 2.0, 6.0		Yamanaka 2002

Glass Composition	Melting Point (°C)	Sintering Temp (°C)	Softening Temp (T_f °C)	Transition Temp (T_g °C)	Vitreous/ Crystallizing	Detail Composition	Comments	Citation
Sn-Si-P-Zn-W	800			286		45.9, 6.0, 35.2, 10.9, 2.0		Yamanaka 2002
Sn-Si-P-Zn-B	800			320		42.9, 6.0, 30.2, 10.9, 10.0		Yamanaka 2002
Na-Al-P-Fe-B	817			462		30.2, 14.4, 37.4, 8.3, 9.4		Donald 2006
Na-Al-P-Fe	830			443		34.9, 16.6, 41.3, 7.2	0.18 wt% loss, 28d at 70°C	Donald 2006
Sn-Si-P-Zn	850			260		42.9, 6.0, 37.2, 13.9		Yamanaka 2002
Sn-Si-P-Zn	850			280		37.9, 5.8, 35.4, 20.9		Yamanaka 2002
Sn-Si-P-Zn-B	850			290		42.9-6.0-36.2-10.9-4.0		Yamanaka 2002
Na-Al-P-Fe	860			445		33.2, 15.9, 41.7, 9.2	0.05 wt% loss, 28d at 70°C	Donald 2006
Sn-Si-P-Zn	900			255		52.9, 7.0, 35.2, 4.9		Yamanaka 2002
Pb-B-Si		425	388	321	Vitreous		Ferro CF 8463	Ferro 2017
Pb-Zn-B		450	370	285	Crystallizing		Ferro CF 7575	Ferro 2017
Pb-Zn-B		450	370	310	Crystallizing		Ferro CF 7572	Ferro 2017
Pb-Zn-B		450	415	366	Vitreous		Ferro CF 7555	Ferro 2017
Pb-B-Al-Si		470	447	385	Vitreous		Ferro CF 7570	Ferro 2017
Pb-B-Al		487	427	365	Vitreous		Ferro CF 1417	Ferro 2017
Pb-Si-B-Al		500	425	360	Vitreous		Ferro IP 510	Ferro 2017
Bi-Zn-B		**500**	**440**	**405**	**Crystallizing**	**60.7, 27.8, 11.3**	**Ferro EG 2998**	**Ferro 2017**
Pb-Zn-B		500	470	415	Crystallizing		Ferro EG 2928	Ferro 2017
Bi-Zn-B		505	385	360			Ferro EG 2812	Ferro 2017
Pb-Si-B-Al		505	551	453	Vitreous		Ferro IP 550	Ferro 2017
Pb-Zn-B		530	445	329	Crystallizing		Ferro CF 7578	Ferro 2017
Bi-Zn-B		535	456	420	Crystallizing		Ferro EG 2992	Ferro 2017
Bi-B-Zn-Al-Ba-Te		535	470	441	Crystallizing	20.3, 45.3, 19.4, 2.2, 6.2, 6.6	Sintering temp. <550C	Liu 2012
Pb-Si-B-Al		540	498	417	Vitreous		Ferro IP 530	Ferro 2017
Bi-B-Zn-Al-Ba		545	480	452	Crystallizing	20.3, 45.3, 19.4, 2.2, 6.2	Sintering temp. <550C	Liu 2012
Si-Bi-Zn-B-Sr-Al		550	476	420			Ideal flow 600-700. 3M V2209	3M 2017a
Si-Bi-Zn-B-Sr-Zr		550	484	430			Ideal flow 550-700. 3M V2211	3M 2017a
Bi-Zn-Si-Al		**550**	**505**	**465**	**Vitreous**	**63.4, 7.8, 23.4, 5.4**	**Ferro EG 2922**	**Ferro 2017**
Si-Bi-Sr-Zn-B		550	535	455			Ideal flow 550-700. PN V2289	3M 2017a
Bi-B-Zn-Al-Ba-Sb		551	476	451	Crystallizing	20.3, 45.3, 19.4, 2.2, 6.2, 6.6	Sintering temp. <550C	Liu 2012
Bi-B-Zn-Al-Ba-Ge		553	484	458	Crystallizing	20.3, 45.3, 19.4, 2.2, 6.2, 6.6	Sintering temp. <550C	Liu 2012
Bi-B-Zn-Al-Ba-Si		557	491	467	Crystallizing	20.3, 45.3, 19.4, 2.2, 6.2, 6.6	Sintering temp. <550C	Liu 2012
Bi-Zn-B		560	520	480	Vitreous		Ferro EG 2964	Ferro 2017
Bi-Zn-B		575	386	370	Crystallizing		Ferro EG 3030	Ferro 2017
Bi-Zn-B		580	535	495	Vitreous		Ferro EG 2735	Ferro 2017
Pb-Zn-B-Si		600	513	413	Crystallizing		Ferro CF 7586	Ferro 2017
Zn-Ba-B-Si		600	525	490	Crystallizing		Ferro EG 2742	Ferro 2017
Si-Bi-Sr-Ba-Zn-B		600	552	460			Ideal flow 600-700. 3M V2290	3M 2017a
Zn-B-Si-Li		600	559	489			Ideal flow 600-650. 3M V1558	3M 2017a

Glass Composition	Melting Point (°C)	Sintering Temp (°C)	Softening Temp (T_f °C)	Transition Temp (T_g °C)	Vitreous/ Crystallizing	Detail Composition	Comments	Citation
Bi-Zn-B-Si-La-Al		600	574	501			Ideal flow 600-650. 3M V1467	3M 2017a
Si-Bi-Sr-Ba-Zn-B-Li		600	582	492			Ideal flow 600-700. 3M V2291	3M 2017a
V-Bi-Te		<600	236	272			3M V3046	Brown 2017
Pb-Zn-B		<600	337	288			3M V2811	Brown 2017
V-Pb-Bi		<600		270			3M V3047	Brown 2017
Bi-P-Zn		**<600**				**60, 30, 10**		**Yang 2014**
Bi-P-Ca		**<600**				**60, 30, 10**		**Yang 2014**
Bi-P-Mg		**<600**				**60, 30, 10**		**Yang 2014**
Bi-P-Na		**<600**				**60, 30, 10**		**Yang 2014**
Te-V-Nb			325	280		56, 37, 7		Dumesnil 1993
Pb-Zn-B			330	283			3M 24936	3M 2017b
Pb-Zn-B			334	292			3M 24934	3M 2017b
Pb-Zn-B			337	318			3M 24932	3M 2017b
Pb-Zn-B			340	295			3M 24931	3M 2017b
Pb-Zn-B			341	283			3M 24935	3M 2017b
Pb-Zn-B			345	298			3M 24929	3M 2017b
Zn-P-Nb			348	283		30, 65, 5	Comparable to Zn-B-P	Hormadaly 2006
Pb-Zn-B			364	320			3M 24927	3M 2017b
Te-V-Zr			370			56, 37, 7		Dumesnil 1993
V-P-Te			<400	271		56.7, 19.8, 23.5	High softening at 400	Naito 2011
V-P-Te-Mn			<400	283	Crystallizing	56.7, 19.8, 23.5 (+23.1)	High softening at 400	Naito 2011
V-P-Te-Fe			<400	288	Crystallizing	56.7, 19.8, 23.5 (+11.7)	High softening at 400	Naito 2011
V-P-Te-Ba			<400	290		56.7, 19.8, 23.5 (+12.2)	High softening at 400	Naito 2011
Zn-P-Nb-Na-Bi			414	357		32, 55, 5, 3, 5	Comparable to Zn-B-P	Hormadaly 2006
Zn-P-Nb			432	381		30, 62.5, 7.5	Comparable to Zn-B-P	Hormadaly 2006
Zn-P-Nb-Al			437	360		32, 62, 3, 3	Comparable to Zn-B-P	Hormadaly 2006
Zn-P-Nb-Na-Bi			448	386		32, 55, 5, 3, 5	Comparable to Zn-B-P	Hormadaly 2006
Pb-B-Si			525			85, 10, 5 (+40% quartz)		Jacq 2006
Zn-P-Nb			539	491		30, 60, 10	Comparable to Zn-B-P	Hormadaly 2006
Pb-B-Si			625			85, 10, 5 (+55% quartz)		Jacq 2006
V-P-Te				245	Crystallizing	57.5, 6.7, 35.8		Naito 2011
V-P-Te				313		55.9, 32.5, 11.6	Low softening at 400	Naito 2011
V-P-Te-Sb				315		56.7, 19.8, 23.5 (+6.4)	Low softening at 400	Naito 2011
Bi-B-Zn-Si-Al				450		45, 30, 15, 6, 4		Jacq 2009
Bi-B-Zn-Si-Al				450		50, 25, 5, 6, 4		Jacq 2009
Bi-B-Zn-Si-Al				450		50, 30, 10, 6, 4		Jacq 2009
Bi-B-Zn-Si-Al				475		40, 35, 15, 6, 4		Jacq 2009
Bi-B-Zn-Si-Al				475		45, 35, 10, 6, 4		Jacq 2009
Bi-B-Zn-Si-Al				475		50, 35, 5, 6, 4		Jacq 2009

Glass Composition	Melting Point (°C)	Sintering Temp (°C)	Softening Temp (T_f °C)	Transition Temp (T_g °C)	Vitreous/ Crystallizing	Detail Composition	Comments	Citation
Pb-B-Sr						80, 20 (+20)	0.09 g/m2/day	Erdogan 2014
Pb-B-Sr						80, 20 (+25)	0.21 g/m2/day	Erdogan 2014
Pb-B-Sr						80, 20 (+30)	0.18 g/m2/day	Erdogan 2014
Pb-B-Cs						65, 35 (+20)	34 g/m2/day	Erdogan 2014
Pb-B-Cs						65, 35 (+25)	21 g/m2/day	Erdogan 2014
Pb-B-Cs						65, 35 (+30)	332 g/m2/day	Erdogan 2014

Appendix C. Thermochemical Parameters used in Glass Dissolution Modeling

Technetium Species

TcO4-
charge= -1 ion size= 4.0 A mole wt.= 160.9976
2 elements in species
1.000 Tc 4.000 O

Tc+++
charge= 3 ion size= 8.0 A mole wt.= 97.0000 g
4 species in reaction
1.000 TcO4- -2.000 H2O 4.000 H+
-1.000 O2(aq)
47.3936 47.6316 500.0000 500.0000
500.0000 500.0000 500.0000 500.0000

TcO++
charge= 2 ion size= 5.0 A mole wt.= 112.9994 g
4 species in reaction
3.000 H+ 1.000 TcO4- -1.500 H2O
-.750 O2(aq)
31.3378 31.5163 500.0000 500.0000
500.0000 500.0000 500.0000 500.0000

TcO4--
charge= -2 ion size= 4.0 A mole wt.= 160.9976 g
4 species in reaction
-1.000 H+ 1.000 TcO4- .500 H2O
-.250 O2(aq)
31.7753 31.8348 500.0000 500.0000
500.0000 500.0000 500.0000 500.0000

TcO4---
charge= -3 ion size= 4.0 A mole wt.= 160.9976 g
4 species in reaction
-2.000 H+ 1.000 TcO4- 1.000 H2O
-.500 O2(aq)
63.1841 63.3031 500.0000 500.0000
500.0000 500.0000 500.0000 500.0000

[TcO(OH)2]2
charge= 0 ion size= 4.0 A mole wt.= 294.0280 g
3 species in reaction
-4.000 H+ 2.000 TcO++ 4.000 H2O
.0909 .0909 500.0000 500.0000
500.0000 500.0000 500.0000 500.0000

TcO(OH)2
charge= 0 ion size= 4.0 A mole wt.= 147.0140 g
3 species in reaction
-2.000 H+ 1.000 TcO++ 2.000 H2O
3.3072 3.3072 500.0000 500.0000
500.0000 500.0000 500.0000 500.0000

TcOOH+
charge= 1 ion size= 4.0 A mole wt.= 130.0067 g
3 species in reaction
1.000 TcO++ -1.000 H+ 1.000 H2O
1.1185 1.1185 500.0000 500.0000
500.0000 500.0000 500.0000 500.0000

AgTcO4 type=
formula=
mole vol.= 0.0000 cc mole wt.= 268.8656 g
2 species in reaction
1.000 Ag+ 1.000 TcO4-
-3.2700 -3.2700 -3.2700 -3.2700
500.0000 500.0000 500.0000 500.0000

HTcO4(s) type=
formula=
mole vol.= 0.0000 cc mole wt.= 162.0055 g
2 species in reaction
1.000 H+ 1.000 TcO4-
6.1259 5.9372 5.7119 5.5186
5.3453 5.2286 500.0000 500.0000

KTcO4(s) type=
formula=
mole vol.= 0.0000 cc mole wt.= 200.0959 g
2 species in reaction
1.000 K+ 1.000 TcO4-
-3.0988 -2.2165 -1.2733 -.4644
.2714 .7969 1.1802 1.4345

NaTcO4(s) type=
formula=
mole vol.= 0.0000 cc mole wt.= 183.9874 g
2 species in reaction
1.000 Na+ 1.000 TcO4-
1.5554 1.5554 500.0000 500.0000
500.0000 500.0000 500.0000 500.0000

Tc(c) type=
formula=
mole vol.= 8.4400 cc mole wt.= 97.0000 g
4 species in reaction
1.000 H+ 1.000 TcO4- -.500 H2O
-1.750 O2(aq)
102.3317 93.5863 83.2776 73.6681
63.9181 55.9979 49.3252 43.7136

Tc(OH)2(s) type=
formula=
mole vol.= 0.0000 cc mole wt.= 131.0146 g

4 species in reaction
1.000 Tc+++ -3.000 H+ 2.500 H2O
-.250 O2(aq)
5.2208 5.2803 500.0000 500.0000
500.0000 500.0000 500.0000 500.0000

Tc(OH)3(s) type=
formula=
mole vol.= 0.0000 cc mole wt.= 148.0219 g
3 species in reaction
1.000 Tc+++ 3.000 H2O -3.000 H+
-9.2664 -9.2664 500.0000 500.0000
500.0000 500.0000 500.0000 500.0000

Tc2O7(s) type=
formula=
mole vol.= 85.4300 cc mole wt.= 305.9958 g
3 species in reaction
2.000 TcO4- -1.000 H2O 2.000 H+
13.5276 13.1307 12.6161 12.1240
11.6179 11.2099 500.0000 500.0000

Tc2S7(s) type=
formula=
mole vol.= 0.0000 cc mole wt.= 418.4200 g
4 species in reaction
-8.000 H2O 9.000 H+ 2.000 TcO4-
7.000 HS-
-252.3303 -230.4122 -206.0984 -184.7676
-164.8652 -150.3258 500.0000 500.0000

Tc3O4(s) type=
formula=
mole vol.= 0.0000 cc mole wt.= 354.9976 g
4 species in reaction
3.000 Tc+++ -9.000 H+ 4.500 H2O
-.250 O2(aq)
-19.3547 -19.2952 500.0000 500.0000
500.0000 500.0000 500.0000 500.0000

Tc4O7(s) type=
formula=
mole vol.= 0.0000 cc mole wt.= 499.9958 g
4 species in reaction
2.000 TcO++ -10.000 H+ 2.000 Tc+++
5.000 H2O
-26.0136 -26.0136 500.0000 500.0000
500.0000 500.0000 500.0000 500.0000

TcO2^2H2O(am) type=
formula=
mole vol.= 0.0000 cc mole wt.= 165.0292 g
3 species in reaction
-2.000 H+ 1.000 TcO++ 3.000 H2O
-4.2528 -4.2528 500.0000 500.0000
500.0000 500.0000 500.0000 500.0000

TcO3(s) type=
formula=
mole vol.= 0.0000 cc mole wt.= 144.9982 g
3 species in reaction
1.000 TcO4-- -1.000 H2O 2.000 H+
500.0000 -23.2253 500.0000 500.0000
500.0000 500.0000 500.0000 500.0000

TcOH(s) type=
formula=
mole vol.= 0.0000 cc mole wt.= 112.9994 g
4 species in reaction
-3.000 H+ 1.500 H2O -.250 O2(aq)
1.000 Tc+++
3.3253 3.3848 500.0000 500.0000
500.0000 500.0000 500.0000 500.0000

TcS2(s) type=
formula=
mole vol.= 0.0000 cc mole wt.= 161.1200 g
3 species in reaction
-1.000 H2O 1.000 TcO++ 2.000 HS-
500.0000 -65.9950 500.0000 500.0000
500.0000 500.0000 500.0000 500.0000

TcS3(s) type=
formula=
mole vol.= 0.0000 cc mole wt.= 193.1800 g
4 species in reaction
1.000 TcO4-- 3.000 HS- -4.000 H2O
5.000 H+
500.0000 -119.6846 500.0000 500.0000
500.0000 500.0000 500.0000 500.0000

TcO2
mole wt.= 128.9834 g
3 species in reaction
1.000 H2O 1.000 TcO++ -2.000 H+

Bismuth Species

Bi+
charge= 1 ion size= 0.0 A mole wt.= 208.9800
1 elements in species
1.000 Bi

Bi+++
charge= 3 ion size= 0.0 A mole wt.= 208.9800
1 elements in species
1.000 Bi

Bi(NO3)2+
charge= 1 ion size= 0.0 A mole wt.= 332.9898 g
2 species in reaction
2.000 NO3- 1.000 Bi+++
-2.5000 -2.5000 500.0000 -2.5000
500.0000 500.0000 500.0000 500.0000

```
*    logK=    -2.500000    deltaH=     0.000000 kJ
*    deltaH not known; therefore log K is certain only for 25
deg C

Bi(OH)2+
   charge=   1    ion size=   0.0 A    mole wt.=   242.9946 g
    3 species in reaction
     -2.000 H+          1.000 Bi+++        2.000 H2O
      3.4740    3.4740   500.0000    3.4740
     500.0000   500.0000   500.0000   500.0000
*    logK=    3.474000    deltaH=     0.000000 kJ
*    deltaH not known; therefore log K is certain only for 25
deg C

Bi(OH)3 (aq)
   charge=   0    ion size=   0.0 A    mole wt.=   260.0019 g
    3 species in reaction
     -3.000 H+          1.000 Bi+++        3.000 H2O
      8.9910    8.9910   500.0000    8.9910
     500.0000   500.0000   500.0000   500.0000
*    logK=    8.991000    deltaH=     0.000000 kJ
*    deltaH not known; therefore log K is certain only for 25
deg C

Bi(OH)4-
   charge=  -1    ion size=   0.0 A    mole wt.=   277.0092 g
    3 species in reaction
     -4.000 H+          1.000 Bi+++        4.000 H2O
     21.1880   21.1880   500.0000   21.1880
     500.0000   500.0000   500.0000   500.0000
*    logK=    21.188000    deltaH=     0.000000 kJ
*    deltaH not known; therefore log K is certain only for 25
deg C

BiBr++
   charge=   2    ion size=   0.0 A    mole wt.=   288.8840 g
    2 species in reaction
      1.000 Br-          1.000 Bi+++
     -3.0316   -3.2400   500.0000   -3.6977
     500.0000   500.0000   500.0000   500.0000
*    logK=    -3.240000    deltaH=   -13.000000 kJ

BiBr2+
   charge=   1    ion size=   0.0 A    mole wt.=   368.7880 g
    2 species in reaction
      2.000 Br-          1.000 Bi+++
     -5.5000   -5.5000   500.0000   -5.5000
     500.0000   500.0000   500.0000   500.0000
*    logK=    -5.500000    deltaH=     0.000000 kJ
*    deltaH not known; therefore log K is certain only for 25
deg C

BiBr3 (aq)
   charge=   0    ion size=   0.0 A    mole wt.=   448.6920 g
    2 species in reaction
      3.000 Br-          1.000 Bi+++
     -7.7000   -7.7000   500.0000   -7.7000
     500.0000   500.0000   500.0000   500.0000
*    logK=    -7.700000    deltaH=     0.000000 kJ
*    deltaH not known; therefore log K is certain only for 25
deg C

BiBr4-
   charge=  -1    ion size=   0.0 A    mole wt.=   528.5960 g
    2 species in reaction
      4.000 Br-          1.000 Bi+++
     -9.0000   -9.0000   500.0000   -9.0000
     500.0000   500.0000   500.0000   500.0000
*    logK=    -9.000000    deltaH=     0.000000 kJ
*    deltaH not known; therefore log K is certain only for 25
deg C

BiBr5--
   charge=  -2    ion size=   0.0 A    mole wt.=   608.5000 g
    2 species in reaction
      5.000 Br-          1.000 Bi+++
     -9.9000   -9.9000   500.0000   -9.9000
     500.0000   500.0000   500.0000   500.0000
*    logK=    -9.900000    deltaH=     0.000000 kJ
*    deltaH not known; therefore log K is certain only for 25
deg C

BiCl++
   charge=   2    ion size=   0.0 A    mole wt.=   244.4330 g
    2 species in reaction
      1.000 Cl-          1.000 Bi+++
     -3.3435   -3.6000   500.0000   -4.1634
     500.0000   500.0000   500.0000   500.0000
*    logK=    -3.600000    deltaH=   -16.000000 kJ

BiCl2+
   charge=   1    ion size=   0.0 A    mole wt.=   279.8860 g
    2 species in reaction
      2.000 Cl-          1.000 Bi+++
     -5.0831   -5.5000   500.0000   -6.4155
     500.0000   500.0000   500.0000   500.0000
*    logK=    -5.500000    deltaH=   -26.000000 kJ

BiCl3 (aq)
   charge=   0    ion size=   0.0 A    mole wt.=   315.3390 g
    2 species in reaction
      3.000 Cl-          1.000 Bi+++
     -7.4046   -7.1000   500.0000   -6.4310
     500.0000   500.0000   500.0000   500.0000
*    logK=    -7.100000    deltaH=    19.000000 kJ

BiCl4-
   charge=  -1    ion size=   0.0 A    mole wt.=   350.7920 g
    2 species in reaction
      4.000 Cl-          1.000 Bi+++
     -7.8274   -8.1000   500.0000   -8.6986
     500.0000   500.0000   500.0000   500.0000
*    logK=    -8.100000    deltaH=   -17.000000 kJ

BiI++
   charge=   2    ion size=   0.0 A    mole wt.=   335.8844 g
```

2 species in reaction
1.000 Bi+++ 1.000 I-
-4.4400 -4.4400 500.0000 -4.4400
500.0000 500.0000 500.0000 500.0000
* logK= -4.440000 deltaH= 0.000000 kJ
* deltaH not known; therefore log K is certain only for 25 deg C

BiNO3++
charge= 2 ion size= 0.0 A mole wt.= 270.9849 g
2 species in reaction
1.000 NO3- 1.000 Bi+++
-1.5076 -1.7000 500.0000 -2.1225
500.0000 500.0000 500.0000 500.0000
* logK= -1.700000 deltaH= -12.000000 kJ

BiOH++
charge= 2 ion size= 0.0 A mole wt.= 225.9873 g
3 species in reaction
-1.000 H+ 1.000 Bi+++ 1.000 H2O
1.3986 1.0970 500.0000 .4347
500.0000 500.0000 500.0000 500.0000
* logK= 1.097000 deltaH= -18.810000 kJ

Bi2O3(cr) type=
formula=
mole vol.= 0.0000 cc mole wt.= 465.9728 g
4 species in reaction
-2.000 OH- 5.000 H2O -8.000 H+
2.000 Bi+++
500.0000 43.1360 500.0000 500.0000
500.0000 500.0000 500.0000 500.0000

Bi2S3 type=
formula=
mole vol.= 0.0000 cc mole wt.= 514.1520 g
3 species in reaction
-3.000 H+ 3.000 HS- 2.000 Bi+++
-41.0600 -41.0600 500.0000 -41.0600
500.0000 500.0000 500.0000 500.0000
* logK= -41.060000 deltaH= 0.000000 kJ
* deltaH not known; therefore log K is certain only for 25 deg C

Bi5O7I type=
formula=
mole vol.= 0.0000 cc mole wt.= 1283.8441 g
5 species in reaction
-6.000 OH- 1.000 I- 13.000 H2O
-20.000 H+ 5.000 Bi+++
500.0000 104.4500 500.0000 500.0000
500.0000 500.0000 500.0000 500.0000

BiI type=
formula=
mole vol.= 0.0000 cc mole wt.= 335.8845 g
2 species in reaction
1.000 I- 1.000 Bi+
500.0000 -18.1100 500.0000 500.0000
500.0000 500.0000 500.0000 500.0000

BiI3 type=
formula=
mole vol.= 0.0000 cc mole wt.= 589.6935 g
2 species in reaction
1.000 Bi+++ 3.000 I-
500.0000 -20.9000 500.0000 500.0000
500.0000 500.0000 500.0000 500.0000

BiOBr type=
formula=
mole vol.= 0.0000 cc mole wt.= 304.8834 g
4 species in reaction
1.000 Br- -2.000 H+ 1.000 Bi+++
1.000 H2O
-7.4500 -7.4500 500.0000 -7.4500
500.0000 500.0000 500.0000 500.0000
* logK= -7.450000 deltaH= 0.000000 kJ
* deltaH not known; therefore log K is certain only for 25 deg C

BiOCl type=
formula=
mole vol.= 0.0000 cc mole wt.= 260.4324 g
4 species in reaction
1.000 Cl- -2.000 H+ 1.000 Bi+++
1.000 H2O
-7.8641 -7.8000 500.0000 -7.6592
500.0000 500.0000 500.0000 500.0000
* logK= -7.800000 deltaH= 4.000000 kJ

BiOI type=
formula=
mole vol.= 0.0000 cc mole wt.= 351.8693 g
4 species in reaction
1.000 I- -1.000 H2O 2.000 OH-
1.000 Bi+++
500.0000 -10.0000 500.0000 500.0000
500.0000 500.0000 500.0000 500.0000

Bi2O3
mole wt.= 465.9600 g
3 species in reaction
-6.000 H+ 3.000 H2O 2.000 Bi+++